Volume 1 | Number 1 | Jan 2013 | Pages 1–100

Dalton Transactions

An international journal of inorganic chemistry
www.rsc.org/dalton

ROYAL SOCIETY OF CHEMISTRY

This is an *Accepted Manuscript*, which has been through the Royal Society of Chemistry peer review process and has been accepted for publication.

Accepted Manuscripts are published online shortly after acceptance, before technical editing, formatting and proof reading. Using this free service, authors can make their results available to the community, in citable form, before we publish the edited article. We will replace this *Accepted Manuscript* with the edited and formatted *Advance Article* as soon as it is available.

You can find more information about *Accepted Manuscripts* in the **Information for Authors**.

Please note that technical editing may introduce minor changes to the text and/or graphics, which may alter content. The journal's standard **Terms & Conditions** and the **Ethical guidelines** still apply. In no event shall the Royal Society of Chemistry be held responsible for any errors or omissions in this *Accepted Manuscript* or any consequences arising from the use of any information it contains.

New *p*-tolylimido rhenium(V) complexes with carboxylate-based ligands: synthesis, structures and their catalytic potential in oxidations with peroxides [†]

I. Gryca,[a] B. Machura,[*,a] J. G. Małecki,[a] Lidia S. Shul'pina,[b]

Armando J. L. Pombeiro [c] and Georgiy B. Shul'pin [*,d]

_____

[a] *Department of Crystallography, Institute of Chemistry, University of Silesia, 9th Szkolna St., 40-006 Katowice, Poland. E-mail: basia@ich.us.edu.pl (B. Machura)*
[b] *Nesmeyanov Institute of Organoelement Compounds, Russian Academy of Sciences, Ulitsa Vavilova, dom 28, Moscow 119991, Russia*
[c] *Centro de Química Estrutural, Complexo I, Instituto Superior Técnico, Universidad de Lisboa, Av. Rovisco Pais, 1049-001 Lisboa, Portugal*
[d] *Semenov Institute of Chemical Physics, Russian Academy of Sciences, ulitsa Kosygina, dom 4, Moscow 119991, Russia. E-mail: Shulpin@chph.ras.ru (G. B. Shul'pin)*

<Abstract >

Novel *p*-tolylimido rhenium(V) complexes *trans*-(Cl,Cl)-[Re(p-NC$_6$H$_4$CH$_3$)Cl$_2$(pyz-2-COO)(PPh$_3$)]·MeCN (**1**), *trans*-(Cl,Cl)-[Re(p-NC$_6$H$_4$CH$_3$)Cl$_2$(pyz-2-COO)(PPh$_3$)] (**2**), *trans*-(Br,Br)-[Re(p-NC$_6$H$_4$CH$_3$)Br$_2$(pyz-2-COO)(PPh$_3$)] (**3**), *cis*-(Cl,Cl)-[Re(p-NC$_6$H$_4$CH$_3$)Cl$_2$(ind-3-COO)(PPh$_3$)]·2MeOH (**4**), 2[Re(p-NC$_6$H$_4$CH$_3$)Cl$_2$(ind-3-COO)(PPh$_3$)]·MeCN (**5**), 2[Re(p-NC$_6$H$_4$CH$_3$)Br$_2$(ind-3-COO)(PPh$_3$)]·MeOH (**6**) and 2[Re(p-NC$_6$H$_4$CH$_3$)Br$_2$(ind-3-COO)(PPh$_3$)]·MeCN (**7**) have been obtained in the reactions of [Re(p-NC$_6$H$_4$CH$_3$)X$_3$(PPh$_3$)$_2$] (X =Cl, Br) with pyrazine-2-carboxylic (pyz-2-COOH or PCA) and indazole-3-carboxylic (ind-3-COOH) acids. The compounds were identified by elemental analysis IR, ^{1}H, ^{13}C and ^{31}P NMR spectroscopy and X-ray crystallography. For

deeper understanding structural and bonding properties of the imido rhenium(V) complexes, the calculations at the DFT level were undertaken for *trans*-(Cl,Cl)-[Re(*p*-NC$_6$H$_4$CH$_3$)Cl$_2$(pyz-2-COO)(PPh$_3$)] and *cis*-(Cl,Cl)-[Re(*p*-NC$_6$H$_4$CH$_3$)Cl$_2$(ind-3-COO)(PPh$_3$)]. The complexes **1**, **3**, **4** and **6** exhibited high catalytic activity in oxidation of alkanes with H$_2$O$_2$ and *tert*-butyl hydroperoxide (TBHP) and of alcohols with TBHP. The selectivity parameters measured in the reactions with linear and branched alkanes indicated that the processes with H$_2$O$_2$ or TBHP proceed with the participation of hydroxyl or *tert*-butoxyl radicals, respectively. The composition of isomers from oxygenation of methylcyclohexane corresponds to the existence of some sterical hindrance around the reaction centers.

Introduction

The introduction of β$^-$ emitting isotopes [188]Re and [186]Re in radiotherapy has spawned a widespread scientific interest in the coordination chemistry of rhenium. A fundamental knowledge about the structural and spectroscopic properties, redox activities, and mechanism of ligand substitution reactions is essential to develop new and improved Re radiopharmaceuticals.[1] In this context high-valent rhenium complexes containing a NR^{2-} ligand seem to be especially attractive. The incorporation of functional groups in the organic moiety R may facilitate the linking of the rhenium(V) imido complex to biologically relevant molecules or allow the modification of the organic subtituent R to manipulate the biodistribution of the radiopharmaceutical.[2]

Another area of growing interest for rhenium(V) compounds is their application as homogeneous catalysts in different organic chemistry transformations. With respect to other metal complexes, rhenium compounds offer some advantages as catalysts. Their diverse oxidation states provide a large variety of stable, insensitive to air and moisture complexes, what makes their handling easier for synthetic purposes.[3]

Previously, some of us reported the synthesis and properties of several imidorhenium(V) complexes incorporating monoanionic bidentate N,O-chelating ligands. The compounds [Re(*p*-NC$_6$H$_4$CH$_3$)X$_3$(PPh$_3$)$_2$] (X = Cl, Br) were proven to be useful precursors in the synthesis of imido

compounds. The studies revealed that the geometry of the resulted [Re(p-NC$_6$H$_4$CH$_3$)X$_2$(N–O)(PPh$_3$)]

complexes may be tuned by careful selection of N–O ligands (steric and electronic properties) as well as

experimental conditions. Furthermore, the previous results indicated that different regioisomers of [Re(p-

NC$_6$H$_4$CH$_3$)X$_2$(N–O)(PPh$_3$)] might have a significant influence on their catalyst activity.[4]

To get a deeper understanding of the isomeric preferences in the group of [Re(p-NC$_6$H$_4$CH$_3$)X$_2$(N–

O)(PPh$_3$)] complexes we choose other bidentate chelating carboxylate ligands, pyrazine-2-carboxylic acid

(pyz-2-COOH or PCA) and indazole-3-carboxylic acid (ind-3-COOH). Herein, we present the structural

and spectroscopic properties of the following imido complexes *trans*-(Cl,Cl)-[Re(p-NC$_6$H$_4$CH$_3$)Cl$_2$(pyz-

2-COO)(PPh$_3$)]·MeCN (**1**), *trans*-(Cl,Cl)-[Re(p-NC$_6$H$_4$CH$_3$)Cl$_2$(pyz-2-COO)(PPh$_3$)] (**2**), *trans*-(Br,Br)-

[Re(p-NC$_6$H$_4$CH$_3$)Br$_2$(pyz-2-COO)(PPh$_3$)] (**3**), *cis*-(Cl,Cl)-[Re(p-NC$_6$H$_4$CH$_3$)Cl$_2$(ind-3-

COO)(PPh$_3$)]·2MeOH (**4**), 2[Re(p-NC$_6$H$_4$CH$_3$)Cl$_2$(ind-3-COO)(PPh$_3$)]·MeCN (**5**), 2[Re(p-

NC$_6$H$_4$CH$_3$)Br$_2$(ind-3-COO)(PPh$_3$)]·MeOH (**6**) and 2[Re(p-NC$_6$H$_4$CH$_3$)Br$_2$(ind-3-COO)(PPh$_3$)]·MeCN

(**7**). The catalytic potential of the complexes **1**, **3**, **4** and **6** was studied in oxidation of hydrocarbons and

alcohols with peroxides. Interestingly, compounds **1** and **3** contain anion pyz-2-COO$^-$ (pca$^-$) of pyrazine-

2-carboxylic acid (PCA). Earlier it has been demonstrated that addition of PCA to the reaction solution of

H$_2$O$_2$ and methyltrioxiorhenium (MTO)[5a] as well as complexes of vanadium[5b] or iron[5c] accelerates the

oxidation of alkanes and other organic compounds (see also a review [30d] below specially devoted to PCA

as a co-catalyst and ligand in various oxidations). Preliminary results obtained in this study show that in

some cases these complexes exhibit high activity. More detailed investigations were carried out for

complex **4**.

To elucidate the structural, spectroscopic and bonding properties, calculations at the DFT level

were undertaken for *trans*-(Cl,Cl)-[Re(p-NC$_6$H$_4$CH$_3$)Cl$_2$(pyz-2-COO)(PPh$_3$)] and *cis*-(Cl,Cl)-[Re(p-

NC$_6$H$_4$CH$_3$)Cl$_2$(ind-3-COO)(PPh$_3$)].[6]

Experimental section

Materials. The reagents used to the synthesis were commercially available and were used without further purification. The complexes [Re(p-NC$_6$H$_4$CH$_3$)X$_3$(PPh$_3$)$_2$] (X =Cl, Br) were prepared according to the literature methods.[7]

Instrumentation. Infrared spectra were recorded on a Nicolet Magna 560 spectrophotometer in the spectral range 4000÷400cm^{-1} with the samples in the form of potassium bromide pellets. Electronic spectra were measured on a spectrophotometer Lab Alliance UV-VIS 8500 in the range 1100÷180nm in acetonitrile solution. The ^{1}H NMR, ^{13}C NMR and ^{31}P NMR spectra were recorded (298 K) on Bruker Avance 500 NMR spectrometer at a resonance frequency of 500 MHz for ^{1}H NMR spectra, 125 MHz for ^{13}C NMR spectra and 162 MHz for ^{31}P NMR using DMSO-d$_6$ as solvent and TMS as an internal standard.

General Procedure for the Preparation of Rhenium Complexes 1–7. A mixture of [Re(p-NC$_6$H$_4$CH$_3$)X$_3$(PPh$_3$)$_2$] (0.54 mmol) and the corresponding carboxylic acid (0.60 mmol) in methanol or acetonitrile was refluxed for 4h. The resulting solution was reduced in volume to ~10 ml and allowed to cool to room temperature. A dark brown (complexes **1**–**4**) and green (complexes **5**–**7**) crystalline precipitate was filtered off and dried in the air.

***trans*-(Cl,Cl)-[Re(p-NC$_6$H$_4$CH$_3$)Cl$_2$(pyz-2-COO)(PPh$_3$)]·MeCN (1).** The compound was prepared according to the general procedure by employing pyz-2-COOH (PCA, 0.07 g, 0.60 mmol) and [Re(p-NC$_6$H$_4$CH$_3$)Cl$_3$(PPh$_3$)$_2$] (0.48g, 0.54mmol) in acetonitrile (80 ml). The precipitate was recrystallized from acetonitrile.

C$_{32}$H$_{28}$Cl$_2$N$_4$O$_2$PRe (788.65): calcd. C 48.73, H 3.58, N 7.10%; found C 48.94, H 3.47, N 7.34 %.

IR (KBr; ν/cm^{-1}): 3051(w), 2153(w), 1685(vs), 1590(s), 1482(m), 1435(s), 1414(m), 1299(m), 1277(w), 1158(m), 1095(m), 1055(w), 1017(w), 859(m), 821(m), 790(m), 750(m), 737(sh), 708(sh), 694(s), 649(m), 528(s), 513(w), 499(m), 457(w) and 440(w).

^{1}H NMR (DMSO, ppm): δ = 9.33(s, 1H), 9.05(d, 1H, 3.1Hz), 8.67(d, 1H, 29.4Hz), 8.10(s, 1H), 7.62 – 7.27(m, 16H), 7.19(d, 1H, 8.3Hz), 7.09(d, 1H, 8.4Hz), 2.30(d, 3H, 5.2Hz), 2.08(s, 3H).

^{13}C NMR (125 MHz, DMSO-d$_6$): δ = 167.5, 164.9, 153.8, 147.6, 147.5, 141.9, 140.8, 134.5, 134.1, 133.8,

133.7, 131.1, 131.6, 130.8, 128.5, 128.2, 123.7, 121.6, 30.9, 22.5 ppm.

^{31}P NMR (DMSO-d$_6$): $\delta = 25.50$ ppm.

trans-(Cl,Cl)-[Re(*p*-NC$_6$H$_4$CH$_3$)Cl$_2$(pyz-2-COO)(PPh$_3$)] (2). The compound was prepared according to the general procedure by employing pyz-2-COOH (0.07 g, 0.60 mmol) and [Re(*p*-NC$_6$H$_4$CH$_3$)Cl$_3$(PPh$_3$)$_2$] (0.48g, 0.54mmol) in methanol (80 ml). The precipitate was recrystallized from methanol.

C$_{30}$H$_{25}$Cl$_2$N$_3$O$_2$PRe (747.60): calcd. C 48.20, H 3.37, N 5.62 %; found C 48.51, H 3.42, N 5.49 %.

IR (KBr; ν/cm^{-1}): 3433(br), 3053(w), 1684(vs), 1589(s), 1482(w), 1435(m), 1413(m), 1351(w), 1299(m), 1277(w), 1173(sh), 1158(m), 1095(m), 1056(w), 1017(w), 859(m), 821(w), 790(w), 753(m), 737(sh), 708(sh), 694(s), 649(w), 528(s), 513(w), 491(w) and 457(w).

^{1}H NMR (DMSO, ppm): $\delta = 9.33$(s, 1H), 9.04(d, 1H, 3.1Hz), 8.10(d, 1H, 3.1Hz), 7.61–7.45(m, 17H), 7.29(d, 2H, 8.1Hz), 2.29(s, 3H).

^{13}C NMR (125 MHz, DMSO-d$_6$): $\delta = 164.9, 152.4, 146.7, 146.1, 142.1, 141.2, 139.7, 134.1, 134.0, 131.6, 131.5, 130.5, 129.0, 128.9, 128.6, 123.9, 51.1, 22.3$ ppm.

^{31}P NMR (DMSO-d$_6$): $\delta = 25.61$ ppm.

trans-(Br,Br)-[Re(*p*-NC$_6$H$_4$CH$_3$)Br$_2$(pyz-2-COO)(PPh$_3$)] (3). The compound was prepared according to the general procedure by employing pyz-2-COOH (0.07 g, 0.60 mmol) and [Re(*p*-NC$_6$H$_4$CH$_3$)Br$_3$(PPh$_3$)$_2$] (0.57g, 0.54mmol) in acetonitrile (80 ml). The precipitate was recrystallized from acetonitrile.

C$_{30}$H$_{25}$Br$_2$N$_3$O$_2$PRe (836.52): calcd. C 43.07, H 3.01, N 5.02 %; found C 43.36, H 3.20, N 5.27 %.

IR (KBr; ν/cm^{-1}): 3055(w), 1689(vs), 1589(s), 1482(w), 1434(m), 1413(m), 1344(w), 1303(m), 1172(m), 1153(m), 1098(w), 1054(w), 860(m), 823(w), 740(m), 692(s), 649(m), 529(s), 512(m), 487(m), 463(w), and 439(w).

^{1}H NMR of **1** (DMSO, ppm): $\delta = 9.33$(s, 1H), 9.05(dd, 1H, 6.1Hz and 3.2Hz), 8.17 – 8.10(m, 1H), 7.66 – 7.45(m, 17H), 7.30(d, 2H, 8.1Hz), 2.31(s, 3H)

^{13}C NMR (125 MHz, DMSO-d$_6$): $\delta = 167.5, 153.7, 150.3, 147.1, 142.2, 142.9, 134.6, 131.7, 131.5, 131.1,$

130.8, 128.9, 122.4, 30.9, 22.2 ppm.

^{31}P NMR (DMSO-d$_6$): δ = 25.85 ppm.

cis-(Cl,Cl)-[Re(p-NC$_6$H$_4$CH$_3$)Cl$_2$(ind-3-COO)(PPh$_3$)]·2MeOH (4). The compound was prepared according to the general procedure by employing ind-3-COOH (0.07 g, 0.60 mmol) and [Re(p-NC$_6$H$_4$CH$_3$)Cl$_3$(PPh$_3$)$_2$] (0.48g, 0.54mmol) in methanol (80 ml).The precipitate was recrystallized from methanol.

C$_{35}$H$_{35}$Cl$_2$N$_3$O$_4$PRe (849.73): calcd. C 49.47, H 4.15, N 4.94 %; found C 49.62, H 4.21, N 5.08 %.

IR (KBr; ν/cm^{-1}): 3053(w), 2251(w), 1646(vs), 1591(m), 1481(w), 1453(w), 1435(s), 1380(w), 1350(w), 1271(m), 1222(m), 1186(sh), 1174(w), 1153(w), 1126(w), 1095(m), 1067(w), 1018(w), 818(m), 794(w), 749(s), 696(s), 649(m), 529(s), 512(m), 495(m), 449(sh) and 436(m).

^{1}H NMR (DMSO, ppm): δ = 14.29(s, 1H), 7.65(d, 1H, 8.3Hz), 7.50(d, 1H, 7.9Hz), 7.44 – 7.35(m, 6H), 7.34 – 7.19(m, 11H), 7.11(d, 4H, 8.2Hz), 3.17(s, 6H), 2.25(s, 3H).

^{13}C NMR (125 MHz, DMSO-d$_6$): δ = 165.3, 156.9, 154.7, 139.2, 134.1, 132.0, 130.4, 129.5, 128.4, 125.5, 121.9, 119.4, 118.4, 114.6, 51.2, 22.3 ppm.

^{31}P NMR (DMSO-d$_6$): δ = 25.18 ppm.

cis-(Cl,Cl)-2[Re(p-NC$_6$H$_4$CH$_3$)Cl$_2$(ind-3-COO)(PPh$_3$)]·MeCN (5). The compound was prepared according to the general procedure by employing ind-3-COOH (0.07 g, 0.60 mmol) and [[Re(p-NC$_6$H$_4$CH$_3$)Cl$_3$(PPh$_3$)$_2$] (0.43g, 0.54mmol) in acetonitrile (80 ml).The precipitate was recrystallized from acetonitrile.

C$_{68}$H$_{57}$Cl$_4$N$_7$O$_4$P$_2$Re$_2$ (1612.35): calcd. C 50.65, H 3.56, N 6.08 %; found C 50.87, H 3.75, N 6.21 %.

IR (KBr; ν/cm^{-1}): 3053(w), 2251(w), 1646(vs), 1591(m), 1481(w), 1453(w), 1435(s), 1379(w), 1350(w), 1272(m), 1222(m), 1173(w), 1153(w), 1126(w), 1095(m), 1067(w), 1018(w), 818(m), 750(s), 696(s), 647(m), 529(s), 513(m), 496(m), 449(sh) and 436(m).

^{1}H NMR (DMSO, ppm): δ = 14.30(s, 1H), 7.65(d, 1H, 8.4Hz), 7.51(d, 1H, 7.9Hz), 7.44 – 7.36(m, 6H), 7.35 – 7.18(m, 11H), 7.09(q, 4H, 8.3Hz), 2.25(s, 3H), 2.08(s, 1.5H).

^{13}C NMR (125 MHz, DMSO-d$_6$): δ = 162.6, 154.6, 141.7, 135.7, 133.9, 131.5, 130.3, 129.7, 128.9, 125.2,

123.4, 119.6, 118.9, 31.2, 22.1, 1.6 ppm.

^{31}P NMR (DMSO-d$_6$): δ = 25.45 ppm.

cis-(Br,Br)-2[Re(p-NC$_6$H$_4$CH$_3$)Br$_2$(ind-3-COO)(PPh$_3$)]·MeOH (6): The compound was prepared according to the general procedure by employing ind-3-COOH (0.07 g, 0.60 mmol) and [Re(p-NC$_6$H$_4$CH$_3$)Cl$_3$(PPh$_3$)$_2$] (0.57g, 0.54mmol) in methanol (80 ml).The precipitate was recrystallized from methanol.

C$_{67}$H$_{58}$Br$_4$N$_6$O$_5$P$_2$Re$_2$ (1781.17): calcd. C 45.18, H 3.28, N 4.72 %; found C 45.29, H 3.33, N 4.61 %.

IR (KBr; ν/cm^{-1}): 3053(w), 2251(w), 1646(vs), 1591(m), 1481(w), 1435(m), 1350(w), 1270(m), 1220(m), 1124(w), 1094(m), 817(m), 749(s), 708(sh), 696(m), 646(w), 528(s), 512(w), 496(w) and 456(w).

^{1}H NMR (DMSO, ppm): δ = 14.42(s, 1H), 7.67(d, 1H, 8.4Hz), 7.50(d, 1H, 8.1Hz), 7.46 – 7.37(m, 6H), 7.36 – 7.18(m, 10H), 7.12(dd, 4H, 20.3Hz and 8.3Hz), 2.23(s, 3H), 2.08(s, 3H).

^{13}C NMR (125 MHz, DMSO-d$_6$): δ = 165.5, 156.9, 154.8, 139.4, 134.2, 134.1, 131.3, 130.9, 130.4, 129.5, 128.7, 128.0, 127.9, 125.2, 121.9, 119.4, 118.3, 114.6, 51.2, 22.4 ppm.

^{31}P NMR (DMSO-d$_6$): δ = 25.15 ppm.

cis-(Br,Br)-2[Re(p-NC$_6$H$_4$CH$_3$)Br$_2$(ind-3-COO)(PPh$_3$)]·MeCN (7): The compound was prepared according to the general procedure by employing ind-3-COOH (0.07 g, 0.60 mmol) and [Re(p-NC$_6$H$_4$CH$_3$)Cl$_3$(PPh$_3$)$_2$] (0.57g, 0.54mmol) in acetonitrile (80 ml).The precipitate was recrystallized from acetonitrile.

C$_{68}$H$_{57}$Br$_4$N$_7$O$_4$P$_2$Re$_2$ (1790.19): calcd. C 45.62, H 3.21, N 5.48 %; found C 45.47, H 3.30, N 5.59 %.

IR (KBr; ν/cm^{-1}): 3053(w), 2246(w), 2185(w), 1645(vs), 1590(m), 1480(w), 1451(w), 1435(m), 1384(w), 1350(w), 1270(m), 1220(m), 1185(sh), 1173(w), 1152(w), 1124(w), 1094(m), 1066(w), 1018(w), 998(w), 817(m), 793(sh), 749(s), 695(s), 646(m), 626(w), 528(s), 511(sh), 496(sh) 449(sh) and 435(m).

^{1}H NMR (DMSO, ppm): δ = 14.43(s, 1H), 7.67(d, 1H, 8.5Hz), 7.49(d, 1H, 8.1Hz), 7.44 – 7.38(m, 6H), 7.36 – 7.19(m, 11H), 7.12(dd, 4H, 20.0Hz and 8.3Hz), 2.23(s, 3H), 2.07(s, 1.5H).

^{13}C NMR (125 MHz, DMSO-d$_6$): δ = 162.9, 154.9, 154.7, 141.9, 135.2, 134.0, 133.9, 131.9, 131.6, 130.4,

7

129.8, 129.2, 128.9, 124.9, 123.5, 119.6, 118.9, 118.6, 110.5, 22.4, 1.62 ppm.

^{31}P NMR (DMSO-d$_6$): δ = 25.66 ppm.

Crystal structure determination and refinement. The X-ray intensity data of **1**–**7** were collected on a Gemini A Ultra diffractometer equipped with Atlas CCD detector and graphite monochromated MoK_α radiation (λ = 0.71073Å) at room temperature. Details concerning crystal data and refinement are given in Table S1. Lorentz, polarization and empirical absorption correction using spherical harmonics implemented in SCALE3 ABSPACK scaling algorithm were applied.[8] The structures were solved by the Patterson method and subsequently completed by the difference Fourier recycling. All the non-hydrogen atoms were refined anisotropically using full-matrix, least-squares technique. The hydrogen atoms were treated as „riding" on their parent carbon atoms and assigned isotropic temperature factors equal 1.2 (non-methyl) and 1.5 (methyl) times the value of equivalent temperature factor of the parent atom. The methyl groups were allowed to rotate about their local threefold axis. SHELXS97 and SHELXL97 programs were used for all the calculations.[9] Atomic scattering factors were those incorporated in the computer programs.

Computational Details. The gas phase geometries of *cis*- and *trans*-(Cl,Cl)-[Re(*p*-NC$_6$H$_4$CH$_3$)Cl$_2$(pyz-2-COO)(PPh$_3$)] and *cis*- and *trans* -(Cl,Cl)-[Re(*p*-NC$_6$H$_4$CH$_3$)Cl$_2$(ind-3-COO)(PPh$_3$)] were optimized without any symmetry restrictions in singlet ground-states with the DFT method using the hybrid PBE1PBE functional of GAUSSIAN-03 program package.[10] The calculations were performed using ECP LANL2DZ basis set with an additional *d* and *f* function with the exponent α = 0.3811 and α = 2.033 for rhenium and the standard 6-31G basis set for other atoms. For chlorine, oxygen, nitrogen and phosphorous atoms, diffuse and polarization functions were added.[11] The optimized geometries of *cis*- and *trans*-(Cl,Cl)-[Re(*p*-NC$_6$H$_4$CH$_3$)Cl$_2$(pyz-2-COO)(PPh$_3$)] and *cis*- and *trans*-(Cl,Cl)-[Re(*p*-NC$_6$H$_4$CH$_3$)Cl$_2$(ind-3-COO)(PPh$_3$)] were verified by performing of frequency calculation. The absence of imaginary frequency in the calculated vibrational frequencies ensures that the optimized geometries correspond to true energy minima. For the geometry optimizations the initial X-ray structures were used, and all the subsequent calculations were performed based on optimized geometries. For *trans*-(Cl,Cl)-

[Re(p-NC$_6$H$_4$CH$_3$)Cl$_2$(pyz-2-COO)(PPh$_3$)] and *cis*-(Cl,Cl)-[Re(p-NC$_6$H$_4$CH$_3$)Cl$_2$(ind-3-COO)(PPh$_3$)],

natural bond orbital (NBO) calculations were performed with the NBO code included in Gaussian03.[12]

Oxygenation reactions of alkanes, cyclohexene or cyclohexanol. Catalysts **1**, **3**, **4** and **6** were

used in the form of stock solutions in MeCN. Aliquots of these solutions were added to the reaction

mixtures in oxidation of alkane, cyclohexene of cyclohexanol. The reactions with H$_2$O$_2$ (50% aqueous) or

TBHP (70% aqueous) were typically carried out in air in thermostated Pyrex cylindrical vessels with

vigorous stirring (**CAUTION**: the combination of air or molecular oxygen and H$_2$O$_2$ with organic

compounds at elevated temperatures may be explosive!). The reactions with alkanes or cyclohexene were

stopped by cooling, and typically analyzed twice, i.e., before and after the addition of an excess of solid

PPh$_3$ using the method. developed previously by Shul'pin.[13] In the case of the formation of the

corresponding alkyl hydroperoxides in substantial concentrations, if an excess of solid PPh$_3$ is added to a

sample of the reaction solution, *ca*. 10 min before GC analysis, the alkyl hydroperoxide present is

completely reduced to the corresponding alcohol. As a result, the chromatogram differs from that of a

sample not subjected to the reduction: the alcohol peak rises, while the intensity of the ketone peak

decreases. For precise determination of oxygenate concentrations only data obtained after reduction of the

reaction sample with PPh$_3$ were used. A Perkin-Elmer Clarus 500 gas chromatograph with a BP-20

capillary column (SGE) and Perkin-Elmer Clarus 600 gas chromatograph, equipped with Perkin-Elmer

Clarus 600 C mass-spectrometer (electron impact), with a BPX5 capillary column (SGE) were used for

quantitative and qualitative (MS) analyses of the reaction mixtures. The parameters of all the columns are

30 m $\times$ 0.32 mm $\times$ 25 μm; helium was used as the carrier gas; the internal standard was nitromethane.

Typical chromatograms obtained for the mixtures of products from methylcyclohexane oxidation are

shown in Figure 10.

Results and discussion

Synthesis of the complexes. The complexes *trans*-(Cl,Cl)-[Re(p-NC$_6$H$_4$CH$_3$)Cl$_2$(pyz-2-

COO)(PPh$_3$)]˙MeCN (**1**), *trans*-(Cl,Cl)-[Re(p-NC$_6$H$_4$CH$_3$)Cl$_2$(pyz-2-COO)(PPh$_3$)] (**2**), *trans*-(Br,Br)-

[Re(p-NC$_6$H$_4$CH$_3$)Br$_2$(pyz-2-COO)(PPh$_3$)] (**3**), *cis*-(Cl,Cl)-[Re(p-NC$_6$H$_4$CH$_3$)Cl$_2$(ind-3-

COO)(PPh$_3$)]·2MeOH (**4**), 2[Re(p-NC$_6$H$_4$CH$_3$)Cl$_2$(ind-3-COO)(PPh$_3$)]·MeCN (**5**), 2[Re(p-

NC$_6$H$_4$CH$_3$)Br$_2$(ind-3-COO)(PPh$_3$)]·MeOH (**6**) and 2[Re(p-NC$_6$H$_4$CH$_3$)Br$_2$(ind-3-COO)(PPh$_3$)]·MeCN (**7**)

were prepared in good yield by ligand exchange reactions of [Re(p-NC$_6$H$_4$CH$_3$)X$_3$(PPh$_3$)$_2$] with pyrazine-

2-carboxylic acid (pyz-2-COOH or PCA) and indazole-3-carboxylic acid (ind-3-COOH), respectively

(Scheme 1).
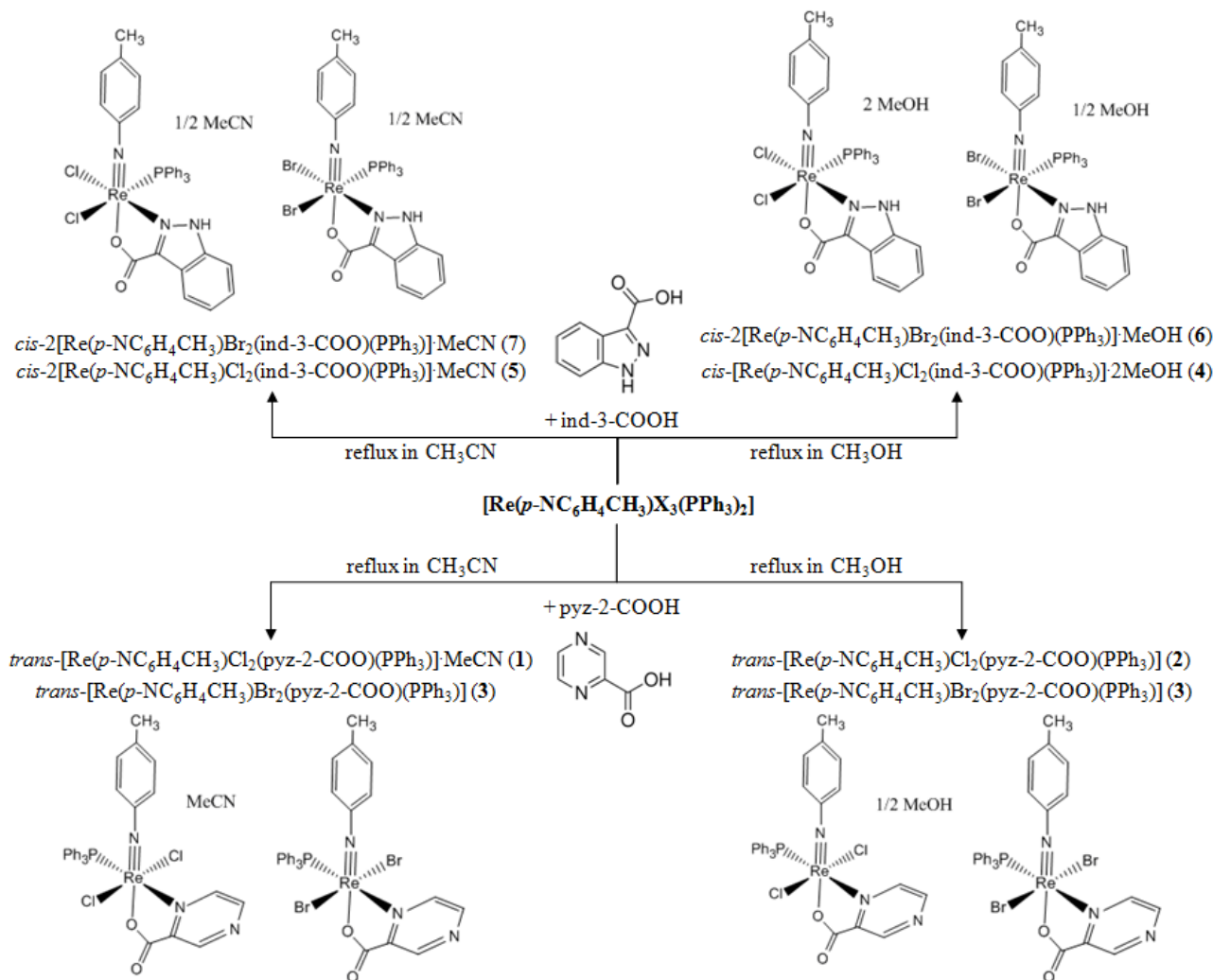
Scheme 1. Formation of complexes **1–7**.

The reactions of [Re(p-NC$_6$H$_4$CH$_3$)X$_3$(PPh$_3$)$_2$] with pyz-2-COOH and ind-3-COOH were

independent of the molar ratio of the precursor to ligand. Even when an excess of the acid was used, only

complexes with one chelating ligand were obtained. Interestingly, refluxing of [Re(p-

NC$_6$H$_4$CH$_3$)X$_3$(PPh$_3$)$_2$] with pyz-2-COOH led to the monosubstituted compounds [Re(p-

NC$_6$H$_4$CH$_3$)X$_2$(pyz-2-COO)(PPh$_3$)] with halide ions in *trans* arrangement, whereas the *cis*-(X,X) isomers were isolated from the reactions of [Re(*p*-NC$_6$H$_4$CH$_3$)X$_3$(PPh$_3$)$_2$] with ind-3-COOH. In contrast to the previously examined reactions of [Re(*p*-NC$_6$H$_4$CH$_3$)X$_3$(PPh$_3$)$_2$] with pyridine-2-carboxylic acid, no different isomeric forms of [Re(*p*-NC$_6$H$_4$CH$_3$)X$_2$(pyz-2-COO)(PPh$_3$)] and [Re(*p*-NC$_6$H$_4$CH$_3$)X$_2$(ind-3-COO)(PPh$_3$)] were obtained under refluxing in methanol and acetonitrile.[4d]

All complexes **1**–**7** show high stability towards air and moisture both in the solid state and in solution for several weeks at ambient temperature. They are moderately soluble in polar solvents such as acetonitrile, acetone, chloroform, dichloromethane and methanol, and in apolar solvents as benzene.

IR and ^{1}H NMR spectra. The IR spectra of **1**–**7** are dominated by a very strong band (at ~1685 cm^{-1} for **1-3** and ~1645 cm^{-1} for **4-7**) assigned to $v_{as}(CO_2)$ stretching mode. Strong $v_s(CO_2)$ bands are found at 1299 and 1277 cm^{-1} for **1**, 1299 and 1277 cm^{-1} for **2**, 1303 and 1285 cm^{-1} for **3**, 1271 and 1222 cm^{-1} for **4**, 1272 and 1222 cm^{-1} for **5**, 1270 and 1220 cm^{-1} for **6** and 1270 and 1220 cm^{-1} for **7**. High values of $\Delta v(CO_2) = v_{as}(CO_2) - v_s(CO_2)$ reflect a unidentate coordination mode of the carboxylate group in compounds **1**–**7**.[14]

In the ^{1}H NMR spectra of the examined compounds distinctive signals corresponding to the alkyl protons of the *p*-tolylimido group occur in the range 3.20–2.00 ppm. The signals at ~ 14.4 ppm indicate the non-deprotonation of the NH group in the indazole-3-carboxylate ligand of **4**–**7**. The aromatic region is dominated by signals of triphenylphosphine protons, which obscure some protons of the imido group.

The coordination of the phosphine was additionally confirmed by ^{31}P NMR spectroscopy. As expected, the single phosphorus signals, observed for **1**–**7** in the 25.15–25.85 ppm range, are downfield from uncoordinated triphenylphosphine (–6 ppm).

The lack of paramagnetic broadening or shifts of resonances in the ^{1}H NMR spectra of **1-7** confirms diamagnetism of the complexes.

Molecular Structures. A definite proof for the structures of **1**–**7** is provided by the X-ray diffraction results. The crystallographic data of **1**–**7** are summarized in Tables S1 and S2.

The perspective drawings of the asymmetric units of the chloro imido complexes are presented in Figure 1, the structural drawings of the bromo analogues are included in Figure S1. The selected bond distances and angles of **1**–**7** are collected in Tables 1 and 2.

All reported complexes show octahedral geometry about the central rhenium atom defined by the *p*-methylphenylimido group, two halide ions, the phosphorus atom of PPh$_3$ molecule, and the carboxylate chelate ligand. Interestingly, the halide ions of **1**–**3** are arranged in *trans* geometry, whereas the halide ligands of **4**–**7** occupy *cis* positions to each other. In all these compounds the oxygen atom of carboxylate ligand occupies *trans* position to the *p*-methylphenylimido ion. This occupancy is justified by *trans*-influence of imido group forcing harder oxygen atom of the N–O ligand into the *trans* position. Triphenylphosphine molecule with its π-acidity adopts *cis* disposition with respect to the linear RN≡Re–O core and stabilizes it due to accessible π-donation from rhenium to PPh$_3$ molecule.

No extraordinary differences in terms of bond lengths and angles can be noticed between *trans*-(X,X)-[Re(*p*-NC$_6$H$_4$CH$_3$)X$_2$(pyz-2-COO)(PPh$_3$)] and *cis*-(X,X)-[Re(*p*-NC$_6$H$_4$CH$_3$)Cl$_2$(ind-3-COO)(PPh$_3$)] compounds (Tables 1 and 2). The Re–N$_{imido}$–C$_{imido}$ bond angles of 173.8(2)° in **1**, 173.6(6)° in **2**, 167.7(7)° in **3**, 167.09(9)° in **4**, 164.05(5)° in **5**, 170.05(6)° in **6** and 168.6(5)° in **7** agree with a linear coordination mode of the arylimido ligands, and they are typical of phenyl imido ligands in high oxidation state complexes, in which the metal is relatively electron-deficient and some π-bonding between the imido nitrogen atom and the metal is likely. The Re–N$_{imido}$ bond lengths, ranging from 1.662(7) to 1.722(4) Å, fall in the range 1.67–1.74Å typical of mononuclear complexes of rhenium(V) having the [Re≡NR]$^{3+}$ core, and reflect the expected triple Re≡N bond.[4,15] The interatomic distance between the rhenium atom and the carboxylate oxygen atom is almost equal to an ideal single Re–O bond length (*ca*. 2.04 Å), indicating lack of delocalization in the RN≡Re–O unit.[16]

For different isomeric preferences in [Re(*p*-NC$_6$H$_4$CH$_3$)X$_2$(pyz-2-COO)(PPh$_3$)] and [Re(*p*-NC$_6$H$_4$CH$_3$)Cl$_2$(ind-3-COO)(PPh$_3$)], the cooperative effect of weak intermolecular interactions seems to

12

be responsible. The crystal structures of **4**–**7** exhibit strong intermolecular N—H•••O hydrogen bonds

(Table S3) between the coordinated indazole ring and oxygen atoms of carboxylate groups and oxygen

atoms of solvate methanol.

A search in the CSD (The Cambridge Structural Database, Version 5.34) reveals 7 *trans*-(X,X)-

isomers and 7 *cis*-(X,X)- isomers, indicating that both isomeric forms are equally observed among

[Re(NR)X$_2$(N–O)(PPh$_3$)] complexes.[17] For complexes [Re(*p*-NC$_6$H$_4$CH$_3$)Cl$_2$(py-2-COO)(PPh$_3$)] and

Re(*p*-NC$_6$H$_4$CH$_3$)X$_2$(quin-2-COO)(PPh$_3$)] both *cis*-X,X and *trans*-X,X isomers were isolated.[4d]

In contrast, the majority of the reported rhenium(V) complexes [ReOX$_2$(N–O)(PPh$_3$)],

incorporating monoanionic bidentate N,O-chelating ligand and oxo ligand isoelectronic to the imido core

NR$^{2–}$, have *cis*-arranged halide ions.[17] A *trans*-X,X conformation has been found only in five complexes

[ReCl$_2$(APO)(PPh$_3$)], [ReOCl$_2$(DPO)(PPh$_3$)] [18] , [ReOX$_2$(hbt)(PPh$_3$)] [19] and [ReOX$_2$(hpb)(PPh$_3$)] [20]

(APOH = 4-anilino-3-penten-2-one; DPOH = 4-[2,6-dimethylanilino]-3-penten-2-one, Hhbt = 2-(2'-

hydroxyphenyl)-2-benzothiazole and Hhpb = 2-(2'-hydroxyphenyl)-1*H*-benzimidazole.

DFT calculations. For further understanding structural and bonding properties of imido

rhenium(V) complexes, the calculations at the DFT level were undertaken for *cis*- and *trans*-(Cl,Cl)-

[Re(*p*-NC$_6$H$_4$CH$_3$)Cl$_2$(pyz-2-COO)(PPh$_3$)] as well as *cis*- and *trans*-(Cl,Cl)-[Re(*p*-NC$_6$H$_4$CH$_3$)Cl$_2$(ind-3-

COO)(PPh$_3$)]. The relative energies and optimized geometries of the *cis*- and *trans* isomers of [Re(*p*-

NC$_6$H$_4$CH$_3$)Cl$_2$(pyz-2-COO)(PPh$_3$)] and [Re(*p*-NC$_6$H$_4$CH$_3$)Cl$_2$(ind-3-COO)(PPh$_3$)] are depicted in Figure

2. For both compounds, *cis* isomers are more stable than *trans* ones, but the energy difference between

them is remarkably small (1.41 kcal mol^{-1} for [Re(*p*-NC$_6$H$_4$CH$_3$)Cl$_2$(pyz-2-COO)(PPh$_3$)] and 1.99 kcal

mol^{-1} for [Re(*p*-NC$_6$H$_4$CH$_3$)Cl$_2$(ind-3-COO)(PPh$_3$)]), indicating that formation of the suitable isomer is

kinetically rather than thermodynamically controlled and can be easily overcome by packing forces.

Formation of isomer *trans* in the reaction [Re(*p*-NC$_6$H$_4$CH$_3$)X$_3$(PPh$_3$)$_2$] with indazole-3-carboxylic acid

seems to be favoured by strong intermolecular N—H•••O hydrogen bonds in the structures **4**–**7** (Table

S1).

As shown in Tables 1 and 2, the PBE1PBE method gives acceptable deviations between the

experimental and theoretical geometric data. The Re–N$_{imido}$ bond lengths are reproduced with deviation of

+0.007 Å for [Re(p-NC$_6$H$_4$CH$_3$)Cl$_2$(pyz-2-COO)(PPh$_3$)] and +0.001 Å for [Re(p-NC$_6$H$_4$CH$_3$)Cl$_2$(ind-3-COO)(PPh$_3$)].

Schematic representation of the energy levels with character of the frontier molecular orbitals of

trans-(Cl,Cl)-[Re(p-NC$_6$H$_4$CH$_3$)Cl$_2$(pyz-2-COO)(PPh$_3$)] and *cis*-(Cl,Cl)-[Re(p-NC$_6$H$_4$CH$_3$)Cl$_2$(ind-3-COO)(PPh$_3$)] is presented in Figure 3. The contours of the selected frontier orbitals are depicted in

Figures 4 and 5, respectively.

The HOMO of these complexes presents significant metallic character and it is mainly constituted

by the rhenium d$_{xy}$ orbital (60%) in antibonding relation to chloride occupied p orbitals (35% and 20%

respectively). For *cis*-(Cl,Cl) isomer, this molecular orbital is also contributed by the chelate ligand

(15%). The HOMO-1 orbital is 1.09 eV for *trans*-(Cl,Cl)-[Re(p-NC$_6$H$_4$CH$_3$)Cl$_2$(pyz-2-COO)(PPh$_3$)] and

0.96 eV for *cis*-(Cl,Cl)-[Re(p-NC$_6$H$_4$CH$_3$)Cl$_2$(ind-3-COO)(PPh$_3$)] lower in energy in relation to the

highest occupied molecular orbital and presents a high contribution of the *p*-methylphenylimido ligand

(65% and 40%, respectively). The contribution of this ligand is due to the interaction of a bonding p

orbital with a metallic d$_\pi$ orbital. To a large extent, the HOMO-1 of *trans*-(Cl,Cl)-[Re(*p*-NC$_6$H$_4$CH$_3$)Cl$_2$(pyz-2-COO)(PPh$_3$)] and *cis*-(Cl,Cl)-[Re(*p*-NC$_6$H$_4$CH$_3$)Cl$_2$(ind-3-COO)(PPh$_3$)] can be

considered as $\pi_{Re\equiv NR}$ orbital. For *cis*-(Cl,Cl) isomer, also a significant contribution from the chelate ligand

(40%) is observed in this molecular orbital. In turn, the HOMO-1 of *trans*-(Cl,Cl)-[Re(*p*-NC$_6$H$_4$CH$_3$)Cl$_2$(pyz-2-COO)(PPh$_3$)] is moderately contributed by triphenylphosphine orbitals (15%). A

contribution of $\pi_{Re\equiv NR}$ interaction is also visible in the HOMO-2 of both complexes, but these orbitals are

predominately localized on triphenylphosphine orbitals (75 %) for *trans*-(Cl,Cl)-[Re(*p*-NC$_6$H$_4$CH$_3$)Cl$_2$(pyz-2-COO)(PPh$_3$)] and chelating ligand (60 %) for *cis*-(Cl,Cl)-[Re(*p*-NC$_6$H$_4$CH$_3$)Cl$_2$(ind-3-COO)(PPh$_3$)]. The other high-lying occupied orbitals of both compounds are

mainly centered on the triphenylphosphine orbitals.

The LUMO of these complexes presents a high contribution of the *p*-methylphenylimido ligand,

mainly from the interaction between the π*-antibonding orbital and d$_\pi$ rhenium orbital. A significant

contribution of $\pi^*_{Re\equiv NR}$ orbitals is also observed in LUMO+2 of *trans*-(Cl,Cl)-[Re(*p*-NC$_6$H$_4$CH$_3$)Cl$_2$(pyz-2-COO)(PPh$_3$)] and and LUMO+1 of *cis*-(Cl,Cl)-[Re(*p*-NC$_6$H$_4$CH$_3$)Cl$_2$(ind-3-COO)(PPh$_3$)]. The LUMO+1 and LUMO+3 of *trans*-(Cl,Cl)-[Re(*p*-NC$_6$H$_4$CH$_3$)Cl$_2$(pyz-2-COO)(PPh$_3$)] and LUMO+2 of *cis*-(Cl,Cl)-[Re(*p*-NC$_6$H$_4$CH$_3$)Cl$_2$(ind-3-COO)(PPh$_3$)] are predominantly composed of antibonding π^* orbital of the carboxylate ligand. The other low-lying unoccupied orbitals are mainly contributed by the π-antibonding triphenylphosphine orbitals.

Table 3 presents the global chemical reactivity indices for complexes **1** and **4**, calculated on the basis of frontier molecular orbitals.

Chemical hardness, approximated by equation (1)

$$\eta = (\text{energy }_{LUMO} - \text{energy }_{HOMO}) / 2 \qquad (1),$$

and associated with the stability and reactivity of a chemical system equals to 1.66 and 1.72 for **1** and **4**, respectively. In a molecule, it measures the resistance to change in the electron distribution or charge transfer.[21] Larger value of η for complex **4** indicates its higher stability (less reactivity) in comparison with **1**.

Similarly, the electronic chemical potential is larger for **4**. Physically, μ describes the escaping tendency of electrons from an equilibrium system, and it is defined as the negative of electronegativity of a molecule [22] and determined using equation (2).

$$\mu = (\text{energy }_{LUMO} + \text{energy }_{HOMO}) / 2 \qquad (2)$$

The global electrophilicity indexes (ω), which measure the propensity or capacity of a species to accept electrons are 5.96 eV for **4** and 5.54 eV for **1**. It is calculated using the electronic chemical potential and chemical hardness as shown in equation (3).

$$\omega = \mu^2 / 2\eta \qquad (3)$$

and determine the stabilization in energy after a system accepts additional amount of electronic charge from the environment. The results indicate that the complex **1** is a stronger electrophile than **4**.[23]

To get a deeper insight into the bond characteristics in *trans*-(Cl,Cl)-[Re(*p*-NC$_6$H$_4$CH$_3$)Cl$_2$(pyz-2-COO)(PPh$_3$)] and *cis*-(Cl,Cl)-[Re(*p*-NC$_6$H$_4$CH$_3$)Cl$_2$(ind-3-COO)(PPh$_3$)], natural bond orbital (NBO)

studies have been performed and the results are presented in Table 4. For both complexes the results of

NBO point to the existence of two Re–NR natural bond orbitals. Both orbitals result from overlapping of

the empty d_{xy} and d_{yz} rhenium orbitals with the occupied p_x and p_z orbitals of the deprotonated nitrogen of

the imido ligand, and they are of π character. Lack of $\sigma_{Re–NR}$ natural orbital indicates a conceivable

predominant Coulomb-type Re–ligand interaction.[24] The nature of Re–NR bonds bonds is in agreement

with the results obtained in previous works regarding analysis of the bonding nature of rhenium imido

complexes.[4]

The triple bond character of Re–N$_{imido}$ in *trans*-(Cl,Cl)-[Re(*p*-NC$_6$H$_4$CH$_3$)Cl$_2$(pyz-2-COO)(PPh$_3$)]

and *cis*-(Cl,Cl)-[Re(*p*-NC$_6$H$_4$CH$_3$)Cl$_2$(ind-3-COO)(PPh$_3$)] is also indicated by the Wiberg bond indices

(Table 5). For both complexes, the Wiberg bond indices of Re(1)–N(2) are over three times larger than

those of Re(1)–N(1). The interactions between the metal atom and carboxylic ligands are predominately

ionic and electrostatic interaction dominates these bondings. The WBIs of the Re(1)–O(2)/O(3) and

Re(1)–N(1)/O(3) bonds are in the range of 0.55−0.62. A greater degree of covalent character is evidenced

by WBIs for bonds between the central ion and halide or phosphine ligands.

Catalytic activity. Various soluble and supported rhenium complexes are known to catalyze the

oxidation reactions of organic compounds with peroxides (usually hydrogen peroxide and *tert*-butyl

hydroperoxide, TBHP).[25] For example, rhenium catalysts (in many cases it was methyltrioxorhenium,

MTO) were used in olefin epoxidations and dihydroxylations[26], Baeyer–Villiger oxidation[27], oxidative

transformations of indigo[28a] , arenes[28b,c] and renewables[28d], functionalization of benzylic C–H bonds[28e-h]

and unactivated C–H bonds of inert alkanes.[5a] Theoretical studies of Re-catalyzed functionalizations have

been reported.[29]

We studied the oxygenation of cyclic, linear and branched alkanes as well as cyclohexene with

H$_2$O$_2$ or TBHP catalysed by complexes **1**, **3**, **4** and **6** in acetonitrile solution under mild conditions

(temperature was 50–70 °C). Kinetic curves of accumulation of oxygenates are shown in Figures 6–9.

The reaction samples were analyzed by GC before and after the addition of an excess of solid PPh$_3$ using

the method developed previously by Shul'pin.[13] The chromatograms differ from that of a sample not

subjected to the reduction, and this testifies the presence of alkyl (or cyclohexenyl) hydroperoxides in the

reaction solutions (Scheme 2). For example, in the cyclooctane oxidation with H_2O_2 after 4 h before the

reduction concentration of cyclooctanone was 0.023 M and cyclooctanol concentration was 0.014 M,

while after the reduction with PPh_3 [cyclooctanone] = 0.002 M and [cyclooctanol] = 0.041 M. In the

cyclohexene oxidation after 2 h [cyclohexenone] = 0.028 M and [cyclohexenol] = 0.011 M before the

reduction, while [cyclohexenone] = 0.002 M and [cyclohexenol] = 0.059 M after the reduction with PPh_3.

After 4 h we obtained: [cyclohexenone] = 0.051 M and [cyclohexenol] = 0.015 M before the reduction

while [cyclohexenone] = 0.004 M and [cyclohexenol] = 0.095 M after the reduction with PPh_3. These

data indicate that in the rhenium-catalyzed oxidation alkyl or alkenyl hydroperoxides are formed in

substantial concentration.[13] For precise determination of concentrations of oxygenates only data obtained

after reduction of the reaction sample with PPh_3 were used as this method allows us to accurately measure

by GC the concentration of the three products (alkyl hydroperoxide, alcohol and ketone).[13]
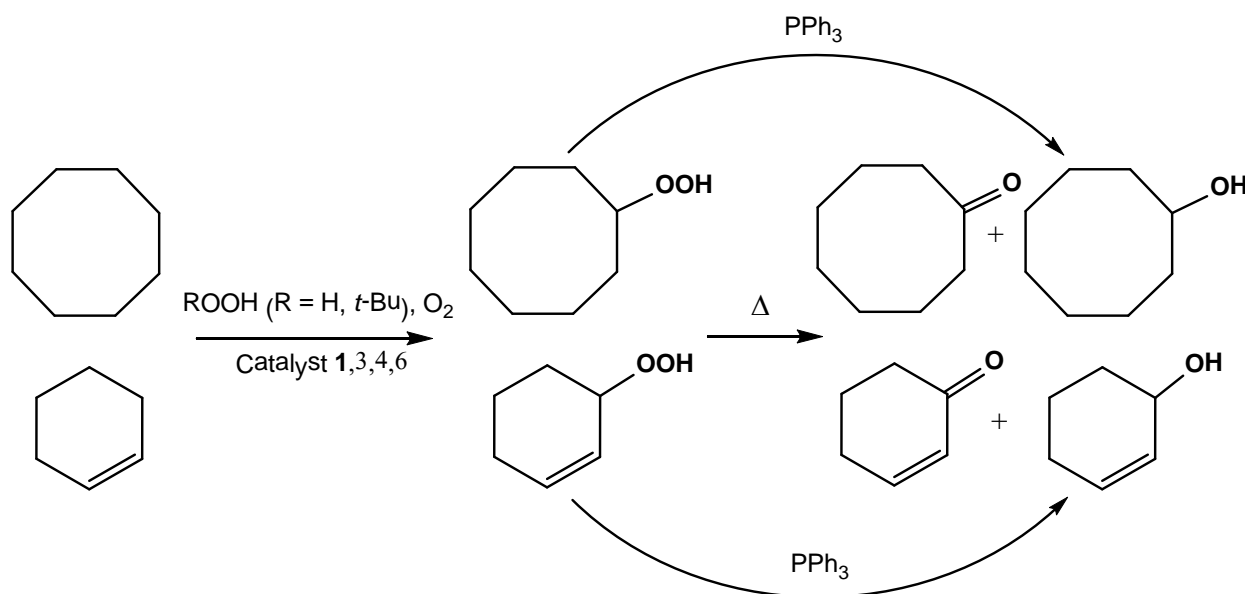
Scheme 2. Transformations of cyclooctane and cyclohexene.

Figure 6 shows that in the **4-**catalyzed oxidation of cyclooctane with hydrogen peroxide

accumulation of oxygenates (mainly cyclooctyl hydroperoxide with minor amounts of cyclooctanol and

cyclooctanone) occurs with pronounced auto-acceleration. This is apparently due to the formation of a

catalytically active species from the starting complex **4** in the initial period of the reaction. Turnover

number (TON, moles of all products per one mol of the catalyst) attained 500 after 6.5 h. We can say that,

although this TON is sufficiently lower than that for oxidation reactions catalyzed by the osmium

complex/pyridine or vanadium complex/pyrazinic acid, it is even higher than TONs reported for certain

iron, copper and rhenium catalysts.[13f,g] Thus, for the catalysis by the MTO–PCA system, the oxidation

with anhydrous H_2O_2 of cyclohexane, cyclooctane and *n*-heptane gave TONs 126, 291 and 134,

respectively.[5a] The reaction of cyclohexane with aqueous H_2O_2 catalyzed by benzoylhydrazido- and -

diazenidorhenium complexes exhibited TONs less that 45.[28i] Maximum TON=270 has been attained in

the cyclohexane oxygenation using trispyrazolylmethane rhenium complexes.[28j] The oxidation with

TBHP (Figure 7) proceeds more slowly in comparison with the reaction with H_2O_2. The yield of all

products in the case of **4** was 27% which is high taking into account the known inertness of alkanes.

Complexes **1**, **3**, **4** and **6** catalyze also the oxidation of cyclohexene with H_2O_2 (Figure 8) or TBHP

(Figure 9). In both cases allylic peroxides are formed which was demonstrated by comparison of

chromatograms before and after reduction of the reaction samples with triphenylphosphine.[13] It is

important to note that the corresponding epoxide is formed in a low concentration (maximum 0.005 M

after 9 h in the reaction shown in Figure 8).

A comparison of kinetic curves for the cyclooctane oxidation with TBHP catalyzed by different

rhenium complexes shown in Fig. 7 demonstrates that compound **4** containing the ind-3-COO ligand

exhibits the highest TON (410) after 10 h, whereas complex **3** bearing the pyz-2-COO (pca) ligand

catalyzes the reaction with the highest initial TOF = 90 h^{-1}. The kinetic curves for catalysis by compounds

1 and **6** practically coincide and this testifies that complexes containing either chlorine or bromine ligands

catalyze the oxidation with similar efficiency. In the oxidation of cyclohexene complexes **4** and **6** are the

most efficient catalysts (Fig. 9). Compounds **1** and **3** exhibit similar activities. Generally, complexes

containing either ind-3-COO or pca ligands on the one hand and either Cl or Br ligands on the other hand

turn out to be catalysts of similar efficiency.

In order to obtain an insight into the mechanism of oxygenation of alkane and allylic C–H bonds with H_2O_2 or TBHP catalyzed by the rhenium complexes we studied the oxidation of some assay alkanes. The results are summarized in Table 6 (for comparison the selectivity parameters measured in the reaction with other oxidizing systems[30] are also given in this Table 6). The value of the regioselectivity parameter for *n*-octane oxidation with the **4**/H_2O_2 system (Entry 1) is low, C(1):C(2):C(3):C(4) ≈ 1:6:6:5. This parameter is similar to the corresponding values for some other systems which oxidize with the participation of hydroxyl radicals and are given in Entries 5–11: the oxidation by hydrogen peroxide in air under UV-irradiation (Entry 5) or in the presence of Fe(II) salt (the Fenton reagent; Entry 6), the oxidation by the H_2O_2/VO_3^-/PCA and the H_2O_2/VO_3^-/H^+ systems (Entries 7 and 8), Os- and Fe-based systems (Entries 9–11). The oxidation with the **1**/H_2O_2 system of *cis*-1,2-DMCH and *trans*-1,2-DMCH, similar to that by reactions shown in entries 5–11, proceeds non-stereoselectively. Unlike all these systems, alkane oxygenation reactions by H_2O_2/[(TMTACN)Mn^{IV}(μ-O)$_3Mn^{IV}$(TMTACN)]$^{2+}$/CH_3COOH system (Entry 15 as well as Entry 16) apparently involve the interaction of the C–H bonds with Mn^V=O species and exhibit much higher selectivity parameters. Selectivity parameters for oxidation with Oxone and *m*-CPBA (Entries 17 and 18, respectively) are noticeably higher than that for the our Re-based systems.

Thus, it follows from Table 6 that the oxidation reactions with H_2O_2 or TBHP catalyzed by the rhenium complexes under discussion exhibit low selectivity parameters for *n*-heptane, a *n*-octane and a branched alkane and the reaction with isomers of 1,2-dimethylcyclohexane is not stereoselective. These data clearly testify that the alkane oxygenation with the **4**/H_2O_2 system proceeds mainly with the participation of free hydroxyl radicals whereas *tert*-butoxyl radicals, *t*-BuO$^\bullet$, are involved into the oxidations by the Re-complex/TBHP systems. A possible role of the ind-3-COO or pca ligands which form 5-membered chelating cycles with rhenium ions (see Scheme 1) is assistance of proton transfer [30a,d,] or stabilization of some transition states [30d,31] in the formation of active radicals.

The oxidation of methylcyclohexane leads to the formation of a set of isomeric ketones and alcohols which relative concentrations were measured after reduction of the reaction samples with triphenylphosphine (Scheme 3). Figure 10 demonstrates examples of chromatograms obtained for the products in Re-catalyzed reactions as well as for comparison in oxidations by some other systems. It can be noticed (Figure 10*a*) that oxidation with the **4**/H_2O_2 system leads to the formation of enhanced amounts of isomers hydroxylated to positions 2 of the cyclohexane ring (products **P6** and **P7**) in comparison with amounts of isomers hydroxylated to position 3 (products **P8** and **P10**). This situation is opposite to that observed for the oxidation by the $Os_3(CO)_{12}$/H_2O_2/py system (Figure 10*b*). In the oxidations with TBHP catalyzed by complexes **4**, **6** and **1** (Figure 10*c*,*d*, and *e*) the peaks of isomers **P6** and **P7** are not higher than peaks of **P8** and **P10**. Amounts of isomers **P6** and **P7** are especially low in the case of catalysis by voluminous complex **6** (Figure 10*d*). It is interesting to compare the obtained here chromatograms with chromatogram (Figure 10*f*) for the oxidation with the very voluminous complex $[O \subset Cu_4\{N(CH_2CH_2O)_3\}_4(BOH)_4][BF_4]_2$ bearing a sterically hindered active centre: in this case isomers **P6** and **P7** are produced in a very low relative concentration.
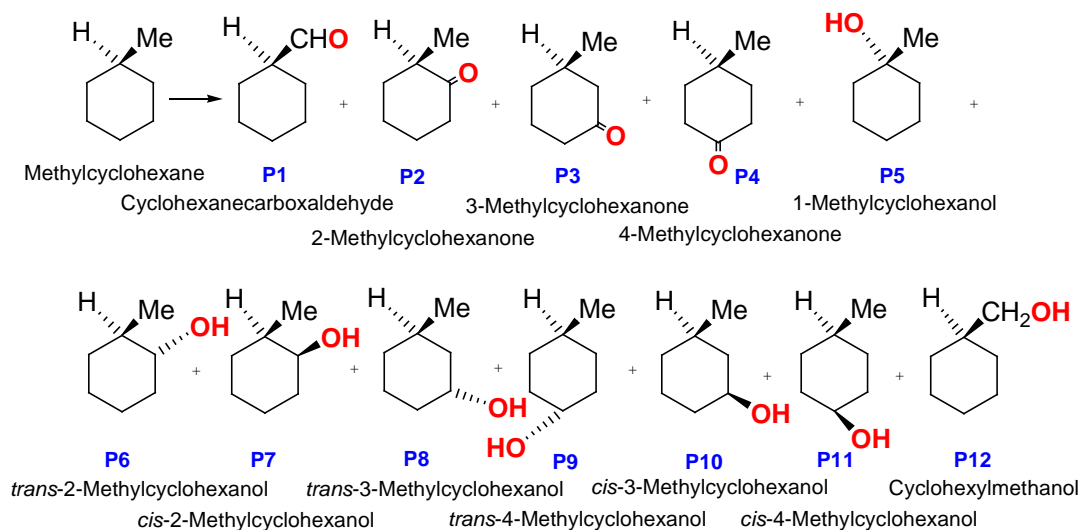
Scheme 3. Products obtained in the oxygenation of methylcyclohexane (after reduction with PPh_3).

20

We have finally found that complex **4** is active as a catalyst in transformation of cyclooctanol to cyclooctanone under the action of TBHP (Figure 11). The reaction occurs in 64% yield, 90% selectivity and TON = 800 after 11 h.

Conclusions

The reactivity of $[Re(p\text{-}NC_6H_4CH_3)Cl_3(PPh_3)_2]$ (X=Cl, Br) towards pyrazine-2-carboxylic and indazole-3-carboxylic acids has been examined. Seven novel rhenium(V) imidocomplexes have been obtained and characterized structurally and spectroscopically. In all of them the carboxylate ligand is coordinated in a chelate way *via* N- and O-donor atoms, and the PPh_3 molecule is *cis*-located in relation to the $Re\equiv N$ moiety, which forces the metal nonbonding *d* electrons to lie in the plane perpendicular to the $M\equiv N$ bond axis. The X-ray studies and NBO analysis confirm a linear coordination mode of the $p\text{-}NC_6H_4CH_3$ ligand and a triple bond between the rhenium and the imido ligand. For *trans*-(Cl,Cl)-[Re(p-NC$_6$H$_4$CH$_3$)Cl$_2$(pyz-2-COO)(PPh$_3$)]·MeCN (**1**), *trans*-(Cl,Cl)-[Re(p-NC$_6$H$_4$CH$_3$)Cl$_2$(pyz-2-COO)(PPh$_3$)] (**2**), *trans*-(Br,Br)-[Re(p-NC$_6$H$_4$CH$_3$)Br$_2$(pyz-2-COO)(PPh$_3$)] (**3**), the halide ions arranged in *trans* geometry, whereas the halide ligands of complexes incorporating indazole-3-carboxylate ligand occupy *cis* positions to each other. For different halide arrangement in [Re(p-NC$_6$H$_4$CH$_3$)X$_2$(pyz-2-COO)(PPh$_3$)] and [Re(p-NC$_6$H$_4$CH$_3$)Cl$_2$(ind-3-COO)(PPh$_3$)], the cooperative effect of weak intermolecular interactions seems to be responsible.

The synthesized complexes exhibited high catalytic activity in oxidation alkanes and hydrocarbons with peroxides. The reactions proceed with the participation of free radicals.

ABBREVIATIONS

pyz-2-COOH or PCA, pyrazine-2-carboxylic acid; pyz-2-COO or pca, pyrazine-2-carboxylate anion; ind-3-COOH, indazole-3-carboxylic acid; ind-3-COO, indazole-3-carboxylate anion; TBHP, *tert*-butyl hydroperoxide (*t*-BuOOH); TON, turnover number (mols of product per mol of catalyst); TOF, turnover frequency (mols of product per mol of catalyst per hour).

Acknowledgements

References

1. (*a*) S. S. Jurisson and J. D. Lydon*, Chem. Rev.*, 1999, **99**, 2205-2218; (*b*) S. Liu and D. S. Edwards, *Chem. Rev.*, 1999, **99**, 2235-2268; (*c*) E. S. Mull, V. J. Sattigeri, A. L. Rodriguez and J. A. Katzenellenbogen, *Bioorg. Med. Chem.*, 2002, **10**, 1381-1398. (*d*) P. Blower, *Dalton Trans.*, 2006, 1705-1711; (*e*) U. Abram and R. Alberto, *J. Braz. Chem. Soc.*, 2006, **17**, 1486-1500.

2. B. Coutinho, D. Dawson, J. R. Dilworth, J. R. Miller, M. Rosser, C. M. Archer and J. D. Kelly, 4, eds. M. Nicolini, G. Bandoli and U. Mazzi, S.G. Editoriali, Padova, **3**, 1995.

3. (*a*) R. Huang and J. H. Espenson, *Inorg. Chem.*, 2001, **40**, 994–999; (*b*) N. Koshino and J. H. Espenson, *Inorg. Chem.*, 2003, **42**, 5735–5742; (*c*) J. Arias, C. R. Newlands and M. M. Abu-Omar, *Inorg. Chem.*, 2001, **40**, 2185–2192; (*d*) M. M. Abu-Omar, *Chem. Commun.*, 2003, 2102–2111; (*e*) L. D. McPherson, M. Drees, S. I. Khan, T. Strassner and M. M. Abu-Omar, *Inorg. Chem.*, 2004, **43**, 4036-4050 ; (*f*) P. Gu, W. Wang, Y. Wang and H. Wei, *Organometallics*, 2013, **32**, 47−51; (*g*) J. L. Smeltz, P. D. Boyle and E. A. Ison, *Organometallics,* 2012, **31**, 5994−5997; (*h*) A. J. L. Pombeiro, M. F. C. Guedes da Silva and R. H. Crabtree, "Technetium & Rhenium: Inorganic & Coordination Chemistry", *in* "Encyclopedia of Inorganic Chemistry", 2nd ed. (R.B. King, ed.-in-chief), *Wiley*, *Chichester* 2005, **IX**, 5499-5516.

4. (*a*) B. Machura, M. Wolff and I Gryca, *Inorganica Chimica Acta*, 2011, **370**, 7-17; (*b*) B. Machura, M. Wolff and I. Gryca, *Polyhedron*, 2011, **30**, 142-153; (*c*) B. Machura, I. Gryca and M.

Dalton Transactions Accepted Manuscript

Wolff, *Polyhedron*, 2012, **31**, 128-135; (*d*) B. Machura, I. Gryca, J. G. Małecki, F. Alonso and Y. Moglie, *Dalton Trans.* 2013, Accepted Manuscript, DOI: 10.1039/C3DT52528G

5. (*a*) U. Schuchardt, D. Mandelli and G. B. Shul'pin, *Tetrahedron Lett.*, 1996, **37**, 6487-6490; (*b*) G. B. Shul'pin, D. Attanasio, L. Suber, *J. Catal*., 1993, **142**, 147–152; (*c*) G. V. Nizova, B. Krebs, G. Süss-Fink, S. Schindler, L. Westerheide, L. Gonzalez Cuervo and G. B. Shul'pin, *Tetrahedron*, 2002, **58**, 9231–9237.

6. W. Koch. M.C. Holthausen, A Chemist's Guide to Density Functional Theory, Wiley-VCH, 2000.

7. J. Chatt, J. D. Garforth, N. P. Johnson and G. A. Rowe, *J. Chem. Soc.*, 1964, 1012-1020.

8. CrysAlis RED, Oxford Diffraction Ltd., Version 1.171.33.46, 2003.

9. G.M. Sheldrick, *Acta Cryst.*, 2008, **A64**, 112-122.

10. Gaussian 09, Revision **A.1**, M. J. Frisch, G. W. Trucks, H. B. Schlegel, G. E. Scuseria, M. A. Robb, J. R. Cheeseman, G. Scalmani, V. Barone, B. Mennucci, G. A. Petersson, H. Nakatsuji, M. Caricato, X. Li, H. P. Hratchian, A. F. Izmaylov, J. Bloino, G. Zheng, J. L. Sonnenberg, M. Hada, M. Ehara, K. Toyota, R. Fukuda, J. Hasegawa, M. Ishida, T. Nakajima, Y. Honda, O. Kitao, H. Nakai, T. Vreven, J. A. Montgomery, Jr., J. E. Peralta, F. Ogliaro, M. Bearpark, J. J. Heyd, E. Brothers, K. N. Kudin, V. N. Staroverov, R. Kobayashi, J. Normand, K. Raghavachari, A. Rendell, J. C. Burant, S. S. Iyengar, J. Tomasi, M. Cossi, N. Rega, J. M. Millam, M. Klene, J. E. Knox, J. B. Cross, V. Bakken, C. Adamo, J. Jaramillo, R. Gomperts, R. E. Stratmann, O. Yazyev, A. J. Austin, R. Cammi, C. Pomelli, J. W. Ochterski, R. L. Martin, K. Morokuma, V. G. Zakrzewski, G. A. Voth, P. Salvador, J. J. Dannenberg, S. Dapprich, A. D. Daniels, O. Farkas, J. B. Foresman, J. V. Ortiz, J. Cioslowski, and D. J. Fox, Gaussian, Inc., Wallingford CT, 2009.

11. (*a*) P. J. Hay and W. R. Wadt, *J. Chem. Phys.*, 1985, **82**, 299-310; (*b*) K. Eichkorn, F. Weigend, O. Treutler and R. Ahlrichs, *Theor. Chem. Acc.*, 1997, **97**, 119-124; (*c*) P. M. W. Gill, B. G. Johnson, J. A. Pople and M. J. Frisch, *Chem. Phys. Lett.*, 1992, **197**, 499-505.

12. (*a*) NBO Version 3.1, E. D. Glendening, A. E. Reed, J. E. Carpenter and F. Weinhold; (*b*) E. Reed, L. A. Curtiss and F. Weinhold, *Chem. Rev.*, 1988, **88**, 899-926.

13. (*a*) G. B. Shul'pin, *J. Mol. Catal., A: Chem.*, 2002, **189**, 39–66; (*b*) G. B. Shul'pin, *Comptes Rendus, Chimie*, 2003, **6**, 163–178; (*c*) G. B. Shul'pin, *Mini-Rev. Org. Chem.*, 2009, **6**, 95–104. (*d*) G. B. Shul'pin, Y. N. Kozlov, L. S. Shul'pina, A. R. Kudinov and D. Mandelli, *Inorg. Chem.*, 2009, **48**, 10480–10482; (*e*) G. B. Shul'pin, Y. N. Kozlov, L. S. Shul'pina and P. V. Petrovskiy, *Appl. Organometal. Chem.*, 2010, **24**, 464–472; (*f*) G. B. Shul'pin, *Dalton Trans.*, 2013, **42**, 12794-12818.

14. G.B. Deacon and R.J. Phillips, *Coord. Chem. Rev.*, 1980, **33**, 227-250.

15. (*a*) J. Gangopadhyay, S. Banerjee, Jiu-Tong Chen and Can-Zhong Lu, *Polyhedron*, 2009, **28**, 2503-2509; (*b*) Samir Das, *Inorg. Chim. Acta*, 2008, **361**, 2815-2820; (*c*) T. I. A. Gerber, D. Luzipo, P. Mayer, *J. Coord. Chem.*, 2006, **59**, 1055-1062; (*d*) P. Mayer, E. Hosten, K. C. Potgieter, T. I. A. Gerber, *J. Chem. Crystallogr.*, 2010, **40**, 1146-1149; (*e*) I. Booysen, T. I. A. Gerber, E. Hosten, P. Mayer, *J. Coord. Chem.*, 2007, **60**, 1749-1753.

16. S. R. Flechter and A. C. Skapski, J. Chem. Soc., *Dalton Trans.*, 1972, 1073-1078.

17. F. H. Allen, *Acta Cryst.*, 2002, **B58**, 380-388.

18. A. Sachse, N. C. Mösch-Zanetti, G. Lyashenko, J. W. Wielandt, K. Most, J. Magull, F. Dall'Antonia, A. Pal and R. Herbst-Irmer, *Inorg. Chem.*, 2007, **46**, 7129-7135.

19. B. Machura, R. Kruszynski and J. Kusz, *Polyhedron*, 2008, **27** 1679-1689.

20. B. Machura and J. Kusz, *Polyhedron*, 2008, **27**, 366-374.

21. (*a*) R. G. Pearson, Hard and soft acids and bases, *Dowden, Hutchinson and Ross, Stroudsberg*, PA, 1973; (*b*) R. G. Pearson, *Acc. Chem. Res.*, 1993, **26**, 250-255; (*c*) R. G. Pearson, Chemical hardness: Application from molecules to solid, *Weinheim: Wiley-VCH*, 1997; (*d*) R. G. Parr and W. Yang, Density functional theory of atoms and molecules, *Oxford: Oxford University Press*, 1989.

22. (*a*) R. G. Parr and R. G. Pearson, *J. Am. Chem. Soc.*, 1983, **105**, 7512; (*b*) P. K. Chattaraj and B. Maiti, *J. Am. Chem. Soc.*, 2003, **125**, 2705-2710.

23. R. G. Parr, L. Szentpaly and S. Liu, *J. Am. Chem. Soc.*, 1999, **121**, 1922-1924.

24. M. L. Kuznetsov, E. A. Klestova-Nadeeva and A. I. Dement'ev, *J. Mol. Struct. (Theochem)*, 2004, **671**, 229-237.

25. (*a*) C. Freund, W. Herrmann and F. E. Kühn, *Top. Organomet. Chem.*, 2007, **22**, 39-77; (*b*) K. R. Jain, W. A. Herrmann and F. E. Kühn, *Coord. Chem. Rev.*, 2008, **252**, 556-568; (*c*) M. Crucianelli, R. Saladino and F. De Angelis, *ChemSusChem*, 2010, **3**, 524-540.

26. (*a*) F. E. Kühn, A. M. Santos and W. A. Herrmann *Dalton Trans*., 2005, 2483-2491; (*b*) A. Sachse, N. C. Mösch-Zanetti, G. Lyashenko, J. W. Wielandt, K. Most, J. Magull, F. Dall'Antonia, A. Pal and R. Herbst-Irmer, *Inorg. Chem*., 2007, **46**, 7129-7135; (*c*) S. Vezzosi, A. G. Ferré, M. Crucianelli, C. Crestini and R. Saladino, *J. Catal.*, 2008, **257**, 262-269; (*d*) C.-J. Qiu, Y.-C. Zhang, Y. Gao and J.-Q. Zhao, *J. Organometal. Chem*., 2009, **694**, 3418-3424; (*e*) R. Saladino, R. Bernini, V. Neri and C. Crestini, *Appl. Catal., A: General*, 2009, **360**, 171-176; (*f*) S. Dinda, M. G. B. Drew and R. Bhattacharyya, *Catal. Commun.*, 2009, **10**, 720-724; (*g*) A. Di Giuseppe, M. Crucianelli, M. Passacantando, S. Nisi and R. Saladino, *J. Catal.*, 2010, **276**, 412-422; (*h*) R. Yang, Y. Zhang and J. Zhao, *Catal. Commun*., 2011, **12**, 923-926; (*i*) K. R. Grünwald, G. Saischek, M. Volpe and N. C. Mösch-Zanetti, *Inorg. Chem*., 2011, **50**, 7162-7171; (*j*) B. Terfassa, P. Traar, M. Volpe, N. C. Mösch-Zanetti, V. J. T. Raju, N. Megersa and N. Retta, *Eur. J. Inorg. Chem.*, 2011, 4434-4440; (*k*) B. Machura, M. Wolff, D. Tabak, J. A. Schachner and N. C. Mösch-Zanetti, *Eur. J. Inorg. Chem.*, 2012, 3764-3773; (*l*) S.-H. Wei and S.-T. Liu, *Catal. Lett*., 2009, **127**, 143-147.

27. (*a*) M.-J. Cheng, S. M. Bischof, R. J. Nielsen, W. A. Goddard III, T. B. Gunnoe and R. A. Periana, *Dalton Trans*., 2012, **41**, 3758-3763; (*b*) E. C. B. A. Alegria, L. M. D. R. S. Martins, M. V. Kirillova and A. J. L. Pombeiro, *Appl. Catal., A: General*, 2012, **443-444**, 27-32; (*c*) L. M. D. R. S. Martins, E. C. B. A. Alegria, P. Smoleński, M. L. Kuznetsov and A. J. L. Pombeiro, *Inorg. Chem.*, 2013, **52**, 4534-4546.

28. (*a*) N. A. F. Al-Rawashdeh, A. M. Al-Ajlouni, S. B. Bukallah and N. Bataineh, *J. Incl. Phenom. Macrocycl. Chem.*, 2011, **70**, 471-480; (*b*) M. Carril, P. Altmann, W. Bonrath, T. Netscher, J.

Schütz and F. E. Kühn, *Catal. Sci. Technol.*, 2012, **2**, 722-724; (*c*) M. Carril, P. Altmann, M. Drees, W. Bonrath, T. Netscher, J. Schütz and F. E. Kühn, *J. Catal.*, 2011, **283**, 55-67; (*d*) T. J. Korstanje and R. J. M. K. Gebbink, *Top. Organomet. Chem.*, 2012, **39**, 129-174; (*e*) R. W. Murray, K. Iyanar, J. Chen and J. T. Wearing, *Tetrahedron Lett.*, 1995, **36**, 6415-6418; (*f*) G. Bianchini, M. Crucianelli, F. De Angelis, V. Neri and R. Saladino, *Tetrahedron Lett.*, 2004, **45**, 2351-2353; (*g*) G. Bianchini, M. Crucianelli, F. De Angelis, V. Neri and R. Saladino, *Tetrahedron Lett.*, 2005, **46**, 2427-2432; (*h*) H. Peng, A. Lin, Y. Zhang, H. Jiang, J. Zhou, Y. Cheng, C. Zhu and H. Hu, *ACS Catal.*, 2012, **2**, 163-167; (*i*) A. M. Kirillov, M. Haukka, M. F. C. G. da Silva and A. J. L. Pombeiro, *Eur. J. Inorg. Chem.*, 2005, 2071-2080; (*j*) E. C. B. Alegria, M. V. Kirillova, L. M. D. R. S. Martins and A. P. L. Pombeiro, *Appl. Catal., A: General*, 2007, **317**, 43-52.

29. (*a*) E. A. Karlsson and T. Privalov, *Chem. Eur. J.*, 2009, **15**, 1862-1869; (*b*) M. L. Kuznetsov and A. J. L. Pombeiro, *Inorg. Chem.*, 2009, **48**, 307–318.

30. (*a*) G. B. Shul'pin, Y. N. Kozlov, G. V. Nizova, G. Süss-Fink, S. Stanislas, A. Kitaygorodskiy and V. S. Kulikova, *J. Chem. Soc., Perkin Trans. 2*, 2001, 1351–1371; (*b*) D. S. Nesterov, E. N. Chygorin, V. N. Kokozay, V. V. Bon, R. Boča, Y. N. Kozlov, L. S. Shul'pina, J. Jezierska, A. Ozarowski, A. J. L. Pombeiro and G. B. Shul'pin, *Inorg. Chem.*, 2012, **51**, 9110–9122; (*c*) J. A. L. da Silva, J. J. R. Fraústo da Silva and A. J. L. Pombeiro, *Coord. Chem. Rev.*, 2011, **255**, 2232-2248; (*d*) A. M. Kirillov and G. B. Shul'pin, *Coord. Chem. Rev.*, 2013, **257**, 732-754; (*e*) L. S. Shul'pina, M. V. Kirillova, A. J. L. Pombeiro and G. B. Shul'pin, *Tetrahedron*, 2009, **65**, 2424–2429; (*f*) G. B. Shul'pin, M. V. Kirillova, Y. N. Kozlov, L. S. Shul'pina, A. R. Kudinov and A. J. L. Pombeiro, *J. Catal.*, 2011, **277**, 164–172; (*g*) G. B. Shul'pin, M. V. Kirillova, L. S. Shul'pina, A. J. L. Pombeiro, E. E. Karslyan and Y. N. Kozlov, *Catal. Commun.*, 2013, **31**, 32–36; (*h*) G. B. Shul'pin, J. Gradinaru and Y. N. Kozlov, *Org. Biomol. Chem.*, 2003, **1**, 3611-3617; (*i*) M. V. Kirillova, Y. N. Kozlov, L. S. Shul'pina, O. Y. Lyakin, A. M. Kirillov, E. P. Talsi, A. J. L. Pombeiro and G. B. Shul'pin, *J. Catal.*, 2009, **268**, 26–38; (*j*) M. V. Kirillova, A. M. Kirillov, D. Mandelli, W. A. Carvalho, A. J. L. Pombeiro and G. B. Shul'pin, *J. Catal.*, 2010, **272**, 9–17; (*k*) A.

M. Kirillov, M. V. Kirillova and A. J. L. Pombeiro, *Adv. Inorg. Chem.*, 2013, **65**, 1-32; (*l*) A. M. Kirillov, M. V. Kirillova, L. S. Shul'pina, P. J. Figiel, K. R. Gruenwald, M. F. C. G. da Silva, M. Haukka, A. J. L. Pombeiro and G. B. Shul'pin, *J. Mol. Catal. A: Chem.*, 2011, **350**, 26–34; (*m*) G. B. Shul'pin, G. Süss-Fink and J. R. Lindsay Smith, *Tetrahedron*, 1999, **55**, 5345–5358; (*n*) V. B. Romakh, B. Therrien, G. Süss-Fink and G. B. Shul'pin, *Inorg. Chem.*, 2007, **46**, 1315–1331; (*o*) G. B. Shul'pin, M. V. Kirillova, Y. N. Kozlov, L. S. Shul'pina, A. R. Kudinov and A. J. L. Pombeiro, *J. Catal.*, 2011, **277**, 164–172; (*p*) G. B. Shul'pin, H. Stoeckli-Evans, D. Mandelli, Y. N. Kozlov, A. Tesouro Vallina, C. B. Woitiski, R. S. Jimenez and W. A. Carvalho, *J. Mol. Catal. A: Chem.*, 2004, **219**, 255–264.

31. (*a*) M. V. Kirillova, M. L. Kuznetsov, V. B. Romakh, L. S. Shul'pina, J. J. R. Fraústo da Silva, A. J. L. Pombeiro and G. B. Shul'pin, *J. Catal.*, 2009, **267**, 140–157; (*b*) M. V. Kirillova, M. L. Kuznetsov, Y. N. Kozlov, L. S. Shul'pina, A. Kitaygorodskiy, A. J. L. Pombeiro and G. B. Shul'pin, *ACS Catal.* 2011, **1**, 1511–1520.

Table 1. The experimental and optimized bond lengths [Å] and angles [°] for **1, 2** and **3.**

	1 (X = Cl)		**2** (X = Cl)	**3** (X = Br)
Bond lengths	Experimental	Optimized	Experimental	Experimental
Re(1)-N(2)	1.702(2)	1.709	1.718(6)	1.716(7)
Re(1)-O(1)	2.0410(19)	2.012	2.063(5)	2.028(6)
Re(1)-N(1)	2.130(2)	2.104	2.129(6)	2.099(8)
Re(1)-X(1)	2.3771(9)	2.396	2.378(2)	2.5064(13)
Re(1)-X(2)	2.4058(9)	2.415	2.404(2)	2.5433(13)
Re(1)-P(1)	2.4317(8)	2.449	2.445(2)	2.429(3)
Re(2)-N(5)			1.706(7)	
Re(2)-O(3)			2.063(6)	
Re(2)-N(4)			2.137(6)	
Re(2)-X(3)			2.401(2)	
Re(2)-X(4)			2.373(2)	
Re(2)-P(2)			2.4507(19)	
Bond angles				
N(2)-Re(1)-O(1)	173.13(10)	172.47	174.6(3)	170.1(3)
N(1)-Re(1)-N(2)	98.48(11)	97.61	103.4(3)	97.0(3)
O(1)-Re(1)-N(1)	75.62(9)	75.97	75.7(2)	75.4(3)
N(1)-Re(1)-X(1)	99.20(9)	98.79	98.9(2)	101.7(2)
O(1)-Re(1)-X(1)	84.30(7)	85.01	86.36(18)	84.2(2)
N(2)-Re(1)-X(1)	88.50(8)	87.54	84.60(18)	84.6(2)
N(1)-Re(1)-X(2)	93.98(9)	92.34	92.2(2)	91.2(2)
O(1)-Re(1)-X(2)	82.04(7)	83.32	82.48(18)	82.3(2)
N(2)-Re(1)-X(2)	84.17(8)	85.54	85.78(18)	88.3(2)
X(1)-Re(1)-X(2)	165.74(3)	167.58	166.77(7)	165.93(5)
N(1)-Re(1)-P(1)	91.84(8)	95.17	91.8(2)	98.5(3)
O(1)-Re(1)-P(1)	94.05(6)	91.30	89.37(16)	89.4(2)
N(2)-Re(1)-P(1)	169.67(7)	167.20	164.67(17)	164.3(2)
X(1)-Re(1)-P(1)	90.34(3)	90.06	90.93(8)	89.64(6)
X(2)-Re(1)-P(1)	94.69(3)	94.42	96.01(8)	94.08(6)
C(25)-N(2)-Re(1)	173.8(2)	170.66	173.6(6)	167.7(7)
N(5)-Re(2)-O(3)			170.9(2)	
N(5)-Re(2)-N(4)			96.1(3)	
O(3)-Re(2)-N(4)			75.7(2)	
N(5)-Re(2)-Cl(4)			100.6(2)	
O(3)-Re(2)-Cl(4)			82.89(17)	
N(4)-Re(2)-Cl(4)			85.25(19)	
N(5)-Re(2)-Cl(3)			92.9(2)	
O(3)-Re(2)-Cl(3)			82.96(17)	
N(4)-Re(2)-Cl(3)			88.10(18)	
Cl(4)-Re(2)-Cl(3)			165.48(9)	
N(5)-Re(2)-P(2)			95.2(2)	
O(3)-Re(2)-P(2)			92.92(15)	
N(4)-Re(2)-P(2)			168.6(2)	
C(54)-N(5)-Re(2)			168.7(5)	

Table 2. The experimental and optimized bond lengths [Å] and angles [°] for **4, 5, 6** and **7.**

	4 (X = Cl)		**5** (X = Cl)	**6** (X = Br)	**7** (X = Br)
Bond lengths	Experimental	Optimized	Experimental	Experimental	Experimental
Re(1)-N(2)	1.706(3)	1.707	1.722(4)	1.692(7)	1.713(4)
Re(1)-O(1)	2.077(3)	2.037	2.092(3)	2.086(6)	2.087(4)
Re(1)-N(1)	2.102(3)	2.086	2.089(4)	2.100(7)	2.086(5)
Re(1)-X(1)	2.3690(11)	2.383	2.3683(14)	2.4949(11)	2.5108(7)
Re(1)-X(2)	2.3953(12)	2.349	2.3961(15)	2.5677(11)	2.5442(7)
Re(1)-P(1)	2.4369(11)	2.453	2.4484(14)	2.443(2)	2.4496(17)
Re(2)-N(5)			1.717(5)	1.698(7)	1.697(5)
Re(2)-O(3)			2.089(4)	2.081(6)	2.094(4)
Re(2)-N(4)			2.079(4)	2.092(7)	2.097(5)
Re(2)-X(3)			2.3545(15)	2.5113(10)	2.4957(8)
Re(2)-X(4)			2.4177(16)	2.5425(11)	2.5685(8)
Re(2)-P(2)			2.4423(15)	2.450(2)	2.4421(17)
Bond angles					
N(2)-Re(1)-O(1)	165.47(14)	161.60	166.12(18)	171.4(3)	166.42(19)
N(1)-Re(1)-N(2)	93.82(14)	89.91	92.10(18)	98.8(3)	92.6(2)
O(1)-Re(1)-N(1)	73.55(12)	73.17	74.13(14)	74.0(2)	73.94(16)
N(1)-Re(1)-X(1)	88.02(10)	84.84	87.21(12)	84.4(2)	87.03(12
O(1)-Re(1)-X(1)	87.11(9)	87.43	83.46(11)	87.04(18)	83.52(11)
N(1)-Re(1)-X(2)	164.94(10)	165.31	167.59(11)	162.99(18)	167.85(12)
N(2)-Re(1)-X(1)	99.85(13)	98.41	97.83(15)	97.0(2)	97.97(16)
O(1)-Re(1)-X(2)	92.06(8)	93.63	94.63(10)	90.63(18)	95.22(11)
N(2)-Re(1)-X(2)	100.99(11)	103.93	99.24(15)	97.1(2)	98.35(16)
X(1)-Re(1)-X(2)	86.78(5)	88.21	86.27(5)	87.54(4)	86.28(2)
N(1)-Re(1)-P(1)	91.47(10)	96.02	90.96(11)	93.3(2)	91.18(13)
O(1)-Re(1)-P(1)	80.39(9)	79.94	80.81(11)	83.02(19)	80.86(12)
N(2)-Re(1)-P(1)	93.05(13)	95.10	98.07(15)	92.9(2)	97.83(17)
X(1)-Re(1)-P(1)	167.09(4)	166.47	164.05(5)	170.04(6)	164.16(4)
X(2)-Re(1)-P(1)	90.46(5)	87.77	92.41(5)	91.98(6)	92.49(4)
C(27)-N(2)-Re(1)	175.2(3)	164.83	169.2(4)	175.8(6	168.6(5)
N(5)-Re(2)-N(4)			97.93(19)	92.5(3)	98.4(2)
N(5)-Re(2)-O(3)			170.49(18)	166.5(3)	170.7(2)
N(4)-Re(2)-O(3)			74.33(16)	74.1(2)	73.90(17)
N(5)-Re(2)-X(3)			98.74(16)	98.5(2)	97.57(17)
N(4)-Re(2)-X(3)			162.48(12)	167.87(18)	163.00(12)
O(3)-Re(2)-X(3)			89.55(11)	95.04(15)	90.69(12)
N(5)-Re(2)-X(4)			98.22(15)	97.9(3)	97.54(17)
N(4)-Re(2)-X(4)			84.68(13)	87.28(18)	84.43(14)
O(3)-Re(2)-X(4)			86.70(11)	83.96(17)	86.96(12)
X(3)-Re(2)-X(4)			87.63(6)	86.17(4)	87.66(3)
N(5)-Re(2)-P(2)			92.06(15)	97.8(3)	92.44(17)
N(4)-Re(2)-P(2)			93.20(13)	91.07(19)	93.36(14)
O(3)-Re(2)-P(2)			83.01(11)	80.57(18)	83.05(12)
X(3)-Re(2)-P(2)			91.56(6)	92.48(6)	91.83(4)
X(4)-Re(2)-P(2)			169.68(5)	164.29(6)	169.99(4)
C(60)-N(5)-Re(2)			177.4(4)	168.5(6)	174.7(5)

Table 3. The global chemical reactivity indices for **1** and **4**.

	1	4
E (Hartree)	–2811,804	–2927,197
LUMO (eV)	–2,79	–2.64
HOMO (eV)	–6.10	–6.08
μ (eV)	–4.44	–4.36
η (eV)	+1.66	+1.72
ω (eV)	+5.96	+5.54

Table 4. The occupancy and composition of the calculated natural bond orbitals (NBOs) between the rhenium and and the p-tolylimido ligand for *trans*-(Cl,Cl)-[Re(p-NC$_6$H$_4$CH$_3$)Cl$_2$(pyz-2-COO)(PPh$_3$)] and *cis*-(Cl,Cl)-[Re(p-NC$_6$H$_4$CH$_3$)Cl$_2$(ind-3-COO)(PPh$_3$)].

BD	Occupancy	Composition of NBO	BD*	Occupancy
trans-(Cl,Cl)-[Re(p-NC$_6$H$_4$CH$_3$)Cl$_2$(pyz-2-COO)(PPh$_3$)]				
Re–N	1.96	0.609(d)$_{Re}$ + 0.793(p)$_N$	0.793(d)$_{Re}$ - 0.609(p)$_N$	0.20
Re–N	1.92	0.657(d)$_{Re}$ + 0.754(p)$_N$	0.754(d)$_{Re}$ - 0.657(p)$_N$	0.24
cis-(Cl,Cl)-[Re(p-NC$_6$H$_4$CH$_3$)Cl$_2$(ind-3-COO)(PPh$_3$)]				
Re–N	1.95	0.623 (d)$_{Re}$ + 0.782 (p)$_N$	0.782 (d)$_{Re}$ - 0.623 (p)$_N$	0.18
Re–N	1.93	0.634 (d)$_{Re}$ + 0.773 (p)$_N$	0.773 (d)$_{Re}$ - 0.634 (p)$_N$	0.27

BD denotes 2-center bond, * - denotes antibond NBO

Table 5. Wiberg bond index matrix in the NAO basis for *trans*-(Cl,Cl)-[Re(p-NC$_6$H$_4$CH$_3$)Cl$_2$(pyz-2-COO)(PPh$_3$)] and *cis*-(Cl,Cl)-[Re(p-NC$_6$H$_4$CH$_3$)Cl$_2$(ind-3-COO)(PPh$_3$)].

Bond	[Re(p-NC$_6$H$_4$CH$_3$)Cl$_2$(pyz-2-COO)(PPh$_3$)]	[Re(p-NC$_6$H$_4$CH$_3$)Cl$_2$(ind-3-COO)(PPh$_3$)]
Re(1)-N(1)	0.557	0.600
Re(1)-N(2)	2.072	2.053
Re(1)-O(1)	0.613	0.606
Re(1)-P(1)	0.776	0.761
Re(1)-Cl(1)	0.883	0.884
Re(1)-Cl(2)	0.856	0.945

30

Table 6. Selectivity parameters obtained in the oxidation of alkanes in acetonitrile catalyzed by rhenium complex and (for comparison) some other systems. [a,b]

Entry	System	C(1):C(2):C(3):C(4)	1°:2°:3°	*trans*:*cis*	
		n-Heptane or *n*-octane	MCH	*cis*-1,2-DMCH	*trans*-1,2-DMCH
1	**4**/H_2O_2 (this work)	1:6:6:5	1:6:19	0.9	0.9
2	**4**/TBHP (this work)	1:10:8:8	1:10:130	0.85	0.85
3	**6**/TBHP (this work)		1:12:200		
4	**1**/TBHP (this work)		1:12:220		
5	hv/H_2O_2 (Ref. 30*a,b*)	1:7:6:7		0.9	
6	$FeSO_4$/H_2O_2 (Ref. 30*a*)	1:5:5:4.5	1:3:6	1.3	1.2
7	(*n*-Bu$_4$N)[VO$_3$]/PCA/H_2O_2 (Ref. 30*a,c,d*)	1:9:7:7	1:6:18	0.75	0.8
8	(*n*-Bu$_4$N)[VO$_3$]/H^+/H_2O_2 (Ref. 30*c,e*)	1:7:7:6.5	1:7:26	0.85	0.9
9	[Os$_3$(CO)$_{12}$]/py/H_2O_2 (Ref. 13*d*)	1:4:4:4	1:5:11		0.85
10	OsCp*$_2$/py/H_2O_2 (Ref. 30*f*)	1:7:7:7	1:8:23	1.0	0.9
11	Cp$_2$Fe/PCA/H_2O_2 (Ref. 30*g*)	1:7:7:6	1:10:33	0.8	0.8
12	[Cu(NCCH$_3$)$_4$]BF$_4$/TBHP (Ref. 30*h*)	1:14:9:13	1:0:40		
13	[O⊂Cu$_4${N(CH$_2$CH$_2$O)$_3$}$_4$(BOH)$_4$][BF$_4$]$_2$/TBHP (Ref. 30*i-k*)	1:34:23:21	1:16:130	0.4	0.1
14	Cu(H$_3$L^1)(NCS)/TBHP (Ref. 30*l*)	1:12:8:7	1:15:150	0.6	0.1
15	[Mn$_2$L$_2$O$_3$]$^{2+}$/MeCO$_2$H/H_2O_2 (Ref. 30*m*)	1:42:37:34	1:26:200	0.34	4.1
16	**"Mn"**/oxalic acid/H_2O_2 (Ref. 30*n*)	1:91:99:68		0.31	13
17	[Mn$_2$L$_2$O$_3$]$^{2+}$/oxalic acid/Oxone (Ref. 30*o*)	1:30:28:30	1:12:150	0.5	0.2
18	FeCl$_3$/L^2/*m*-CPBA (Ref. 30*p*)	1:29:30:27	1:20:210	0.25	3.0

[a] Parameter C(1):C(2):C(3):C(4) is the relative normalized (taking into account the number of hydrogen atoms at each carbon) reactivities of hydrogen atoms at carbons 1, 2, 3 and 4 of the chain of *n*-heptane. Parameter 1°:2°:3° is the relative normalized reactivities of hydrogen atoms at primary, secondary and tertiary carbons of methylcyclohexane (MCH). Parameter *trans*/*cis* is the ratio of isomers of *tert*-alcohols with mutual *trans*- and *cis*-orientation of the methyl groups formed in the oxidation of *cis*- and *trans*-1,2-dimethylcyclohexane (DMCH). All parameters were measured after reduction of the reaction mixtures with triphenylphosphine before GC analysis and calculated based on the ratios of isomeric alcohols.
[b] Abbreviations. Term hv means UV irradiation. Cp$_2$Fe is ferrocene. OsCp*$_2$ is decamethylosmocene. Complex [Mn$_2$L$_2$O$_3$]$^{2+}$ is the binuclear manganese derivative [LMn(μ-O)$_3$MnL]$^{2+}$, where L = 1,4,7-trimethyl-1,4,7-triazacyclononane (TMTACN). Complex **"Mn"** is [Mn$_2$(*R*-L^{Me2R})$_2$(μ-O)$_2$]$^{3+}$ where *R*-L^{Me2R} = (*R*)-1-(2-hydroxypropyl)-4,7-dimethyl-1,4,7-triazacyclononane. Oxone is 2KHSO$_5$.KHSO$_4$.K$_2$SO$_4$. L^2 is tetradentate amine *N*,*N*_-bis(2-pyridylmethylene)-1,4-diaminodiphenyl ether. *m*-CPBA is metachloroperoxybenzoic acid. H$_4$L^1 is N,N,N',N'-tetrakis(2-hydroxyethyl)ethylenediamine.
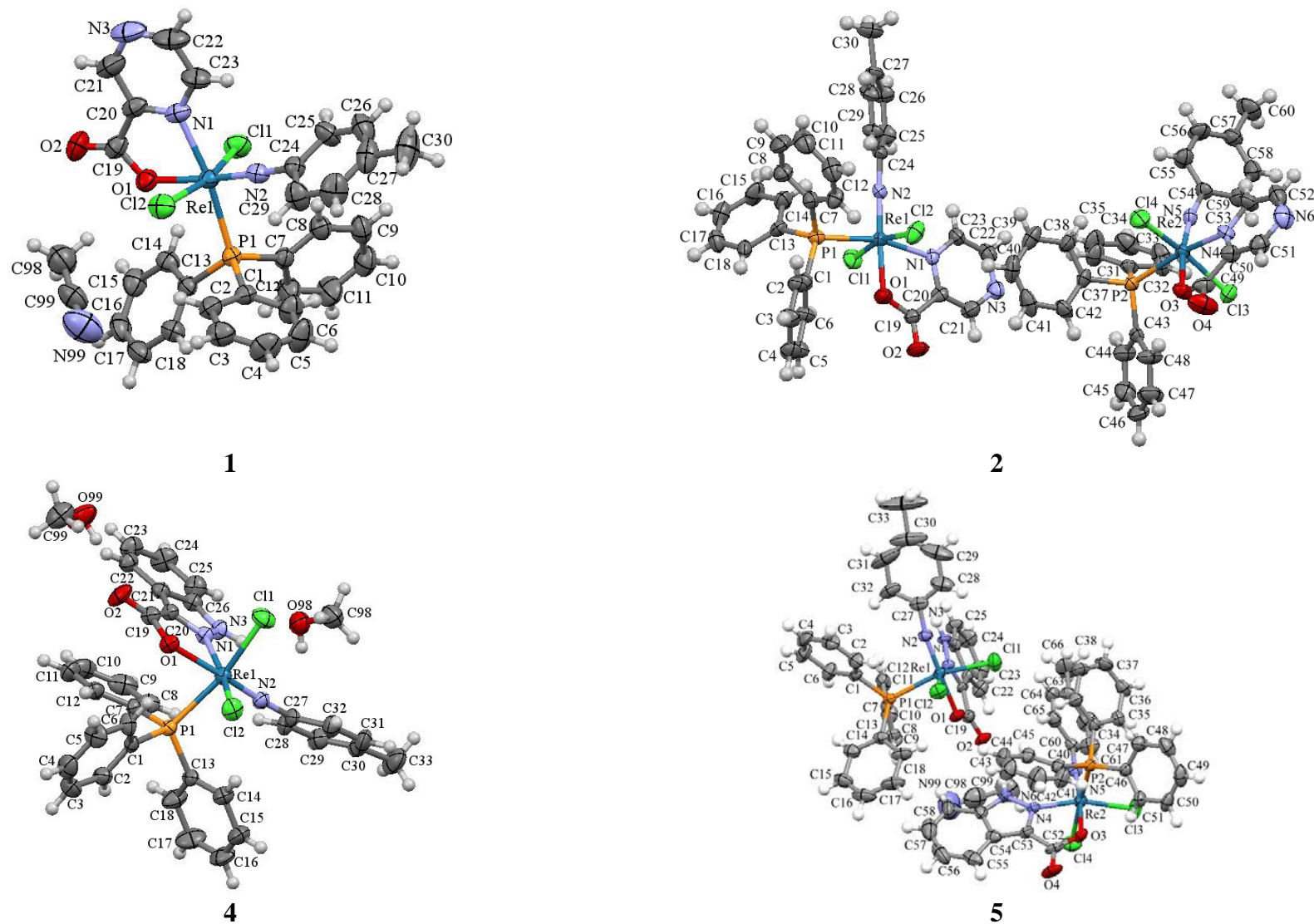
Figure 1. The asymmetric units of the chloro imido rhenium(V) complexes. Displacement ellipsoids are drawn at 50% probability.
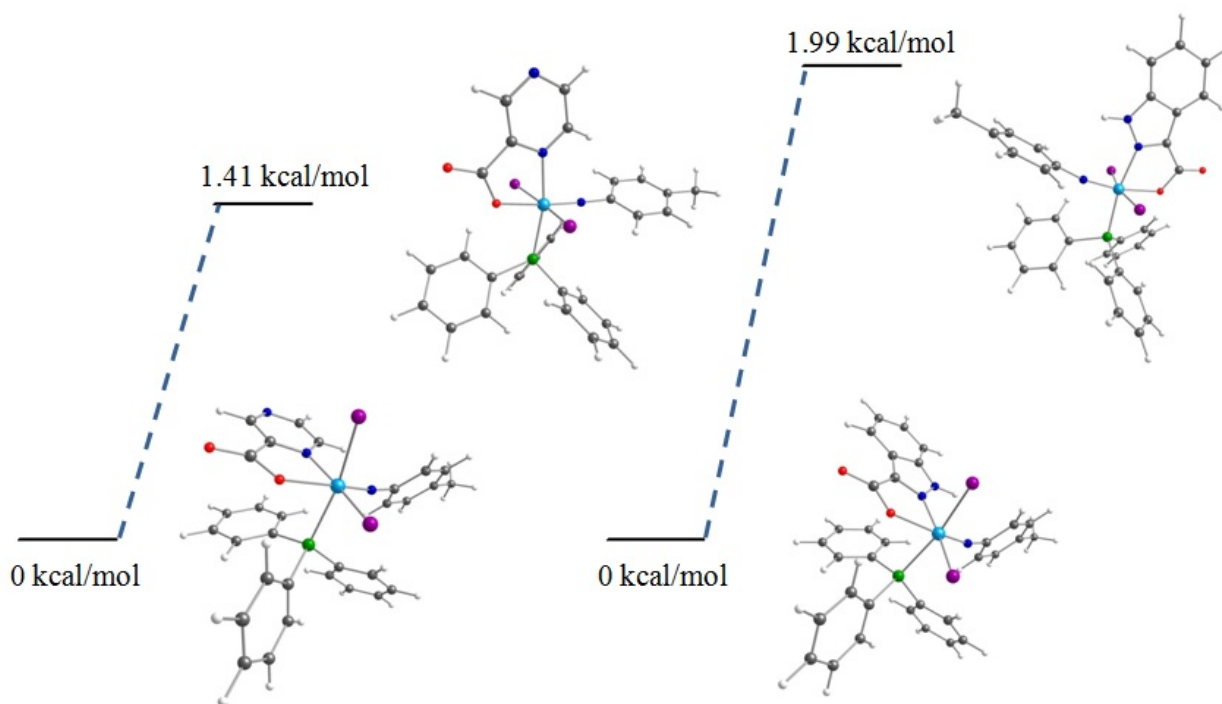
Figure 2. Relative energy (kcal mol^{-1}) diagram for the PBE1PBE-optimized geometries of *cis*- and *trans* isomers of [Re(*p*-NC$_6$H$_4$CH$_3$)Cl$_2$(pyz-2-COO)(PPh$_3$)] and [Re(*p*-NC$_6$H$_4$CH$_3$)Cl$_2$(ind-3-COO)(PPh$_3$)].
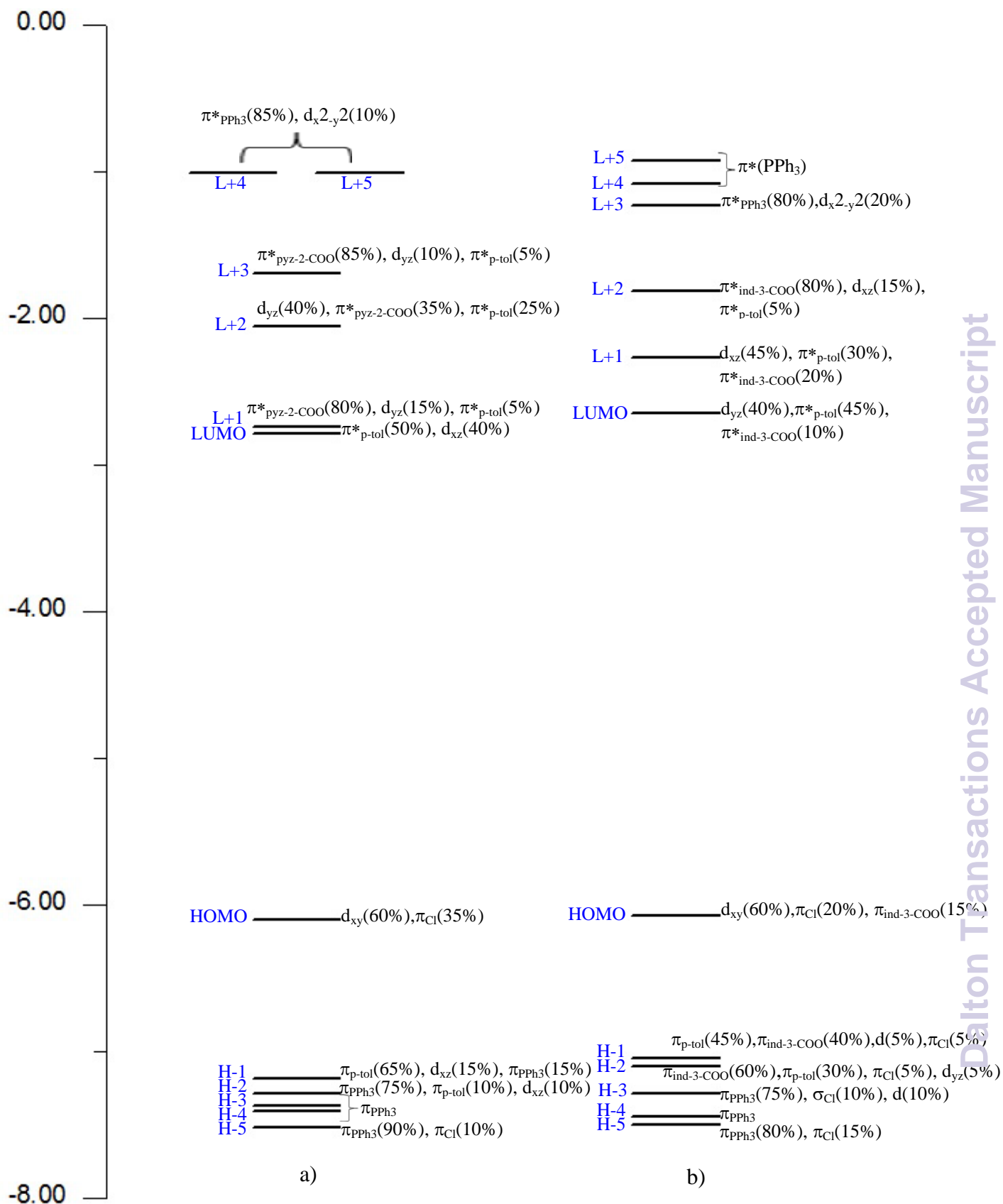
Figure 3. The energy (eV) and character of the occupied and unoccupied molecular orbitals of *trans*-[Re(*p*-NC$_6$H$_4$CH$_3$)Cl$_2$(pyz-2-COO)(PPh$_3$)] (a) and cis-[Re(*p*-NC$_6$H$_4$CH$_3$)Cl$_2$(ind-3-COO)(PPh$_3$)] (b).

Molecular Orbitals of 1

HOMO-2

HOMO-1

HOMO

LUMO

LUMO+1

LUMO+2

LUMO+3

LUMO+4

LUMO+5
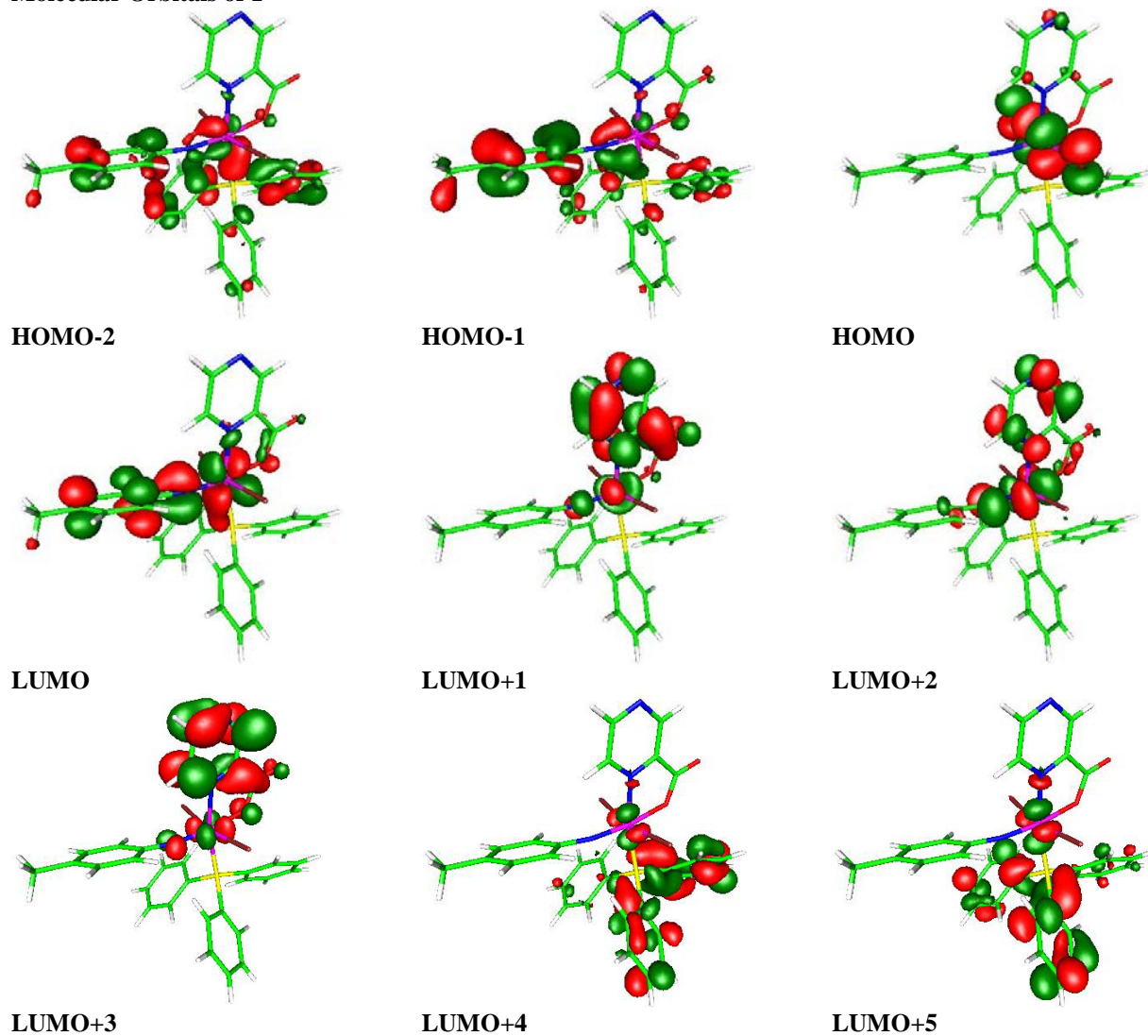
Figure 4. The selected HOMO and LUMO orbitals of *trans*-[Re(*p*-NC$_6$H$_4$CH$_3$)Cl$_2$(pyz-2-COO)(PPh$_3$)]. Positive values of the orbital contour are represented in red (0.04 au) and negative values – in green (–0.04 au).

Molecular Orbitals of 4

HOMO-2   **HOMO-1**   **HOMO**

LUMO   **LUMO+1**   **LUMO+2**

LUMO+3   **LUMO+4**   **LUMO+5**
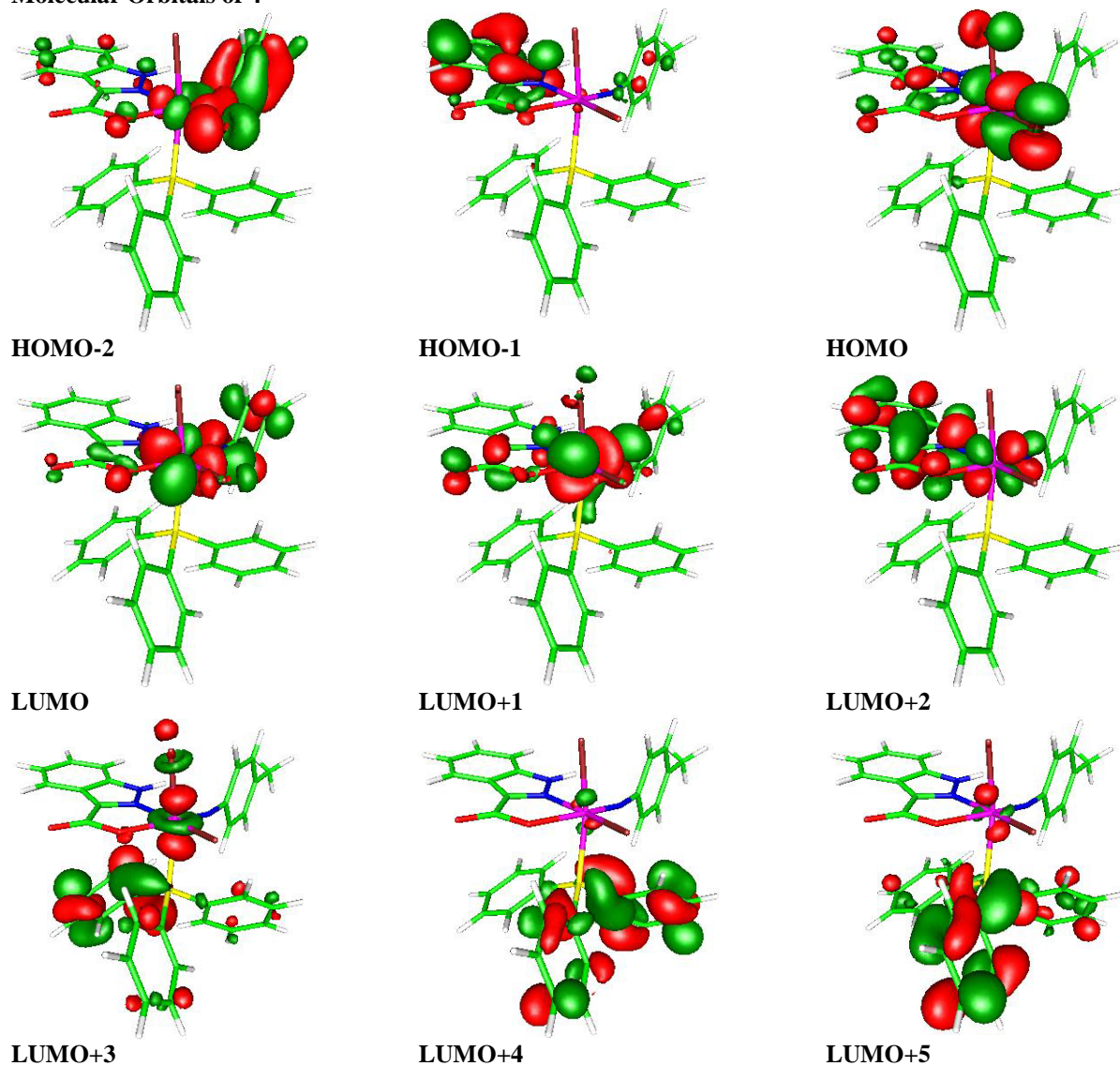
Figure 5. The selected HOMO and LUMO orbitals of cis-[Re(p-NC$_6$H$_4$CH$_3$)Cl$_2$(ind-3-COO)(PPh$_3$)]. Positive values of the orbital contour are represented in red (0.04 au) and negative values – in green (–0.04 au).
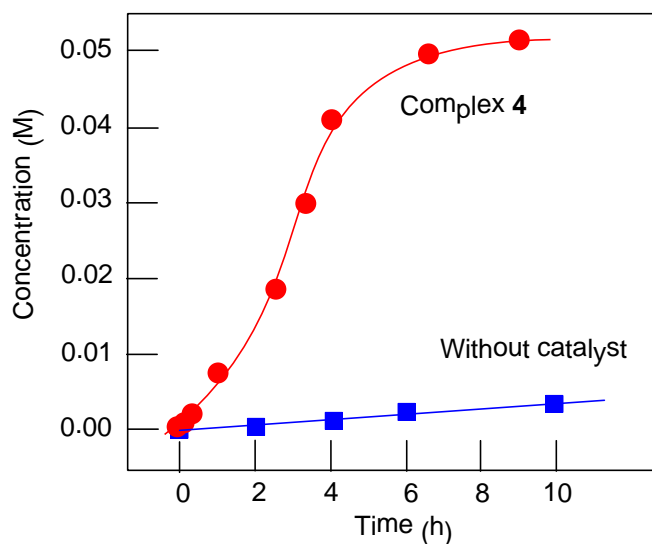
Figure 6. Oxygenation of cyclooctane with the $H_2O_2/4/CH_3CN–H_2O$ system. Kinetic curves of accumulation of oxygenates (predominantly cyclooctyl hydroperoxide) in the presence and in the absence of **4** are shown. Conditions [catalyst **4**]$_0$ = 1.0×10^{-4} M; [H_2O_2]$_0$ = 1.4 M (50% aqueous); [cyclooctane]$_0$ = 0.5 M; MeCN up to total volume 5 mL; 70 °C. Each point corresponds to the sum of concentrations of cyclooctanol and cyclooctanone measured after reduction of the reaction sample with PPh$_3$. After 6.5 h TON = 500 and maximum TOF = 140 h^{-1}.
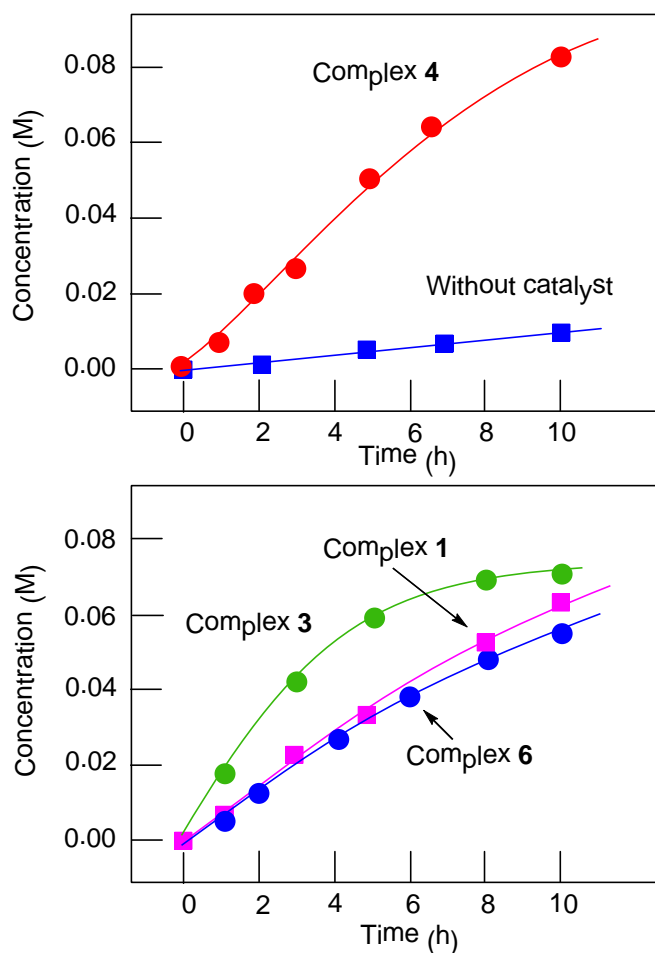
Figure 7. Oxygenation of cyclooctane with the TBHP/Re complex/CH_3CN–H_2O system. Kinetic curves of accumulation of oxygenates (predominantly cyclooctyl hydroperoxide) in the presence and in the absence of complexes **1**, **3**, **4** and **6** are shown. Conditions [Re catalyst]$_0$ = 2.0×10^{-4} M; [TBHP]$_0$ = 1.5 M (70% aqueous); [cyclooctane]$_0$ = 0.3 M; MeCN up to total volume 5 mL; 70 °C. Each point corresponds to the sum of concentrations of cyclooctanol and cyclooctanone measured after reduction of the reaction sample with PPh$_3$. In the reaction catalyzed by **4** TON = 410 after 10 h. The highest initial TOF = 90 h^{-1} was found for the catalysis by **3**.
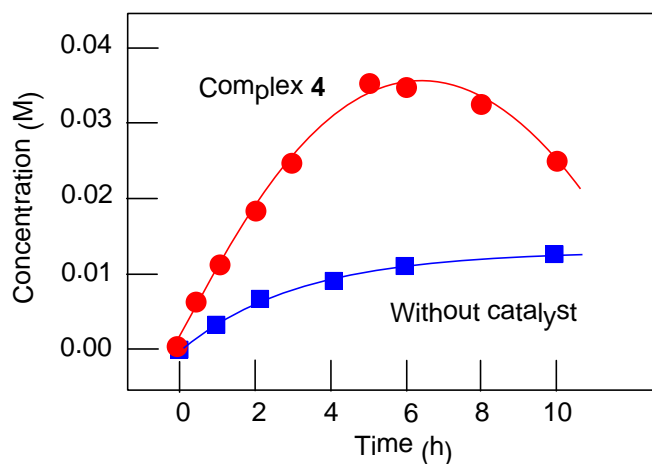
Figure 8. Oxygenation of cyclohexene with the H_2O_2/**4**/CH_3CN–H_2O system. Kinetic curves of accumulation of oxygenates (predominantly cyclohexenyl hydroperoxide) in the presence and in the absence of **4** are shown. Conditions: [catalyst **4**]$_0$ = 2.0×10^{-4} M; [H_2O_2]$_0$ = 2.0 M (50% aqueous); [cyclohexene]$_0$ = 0.3 M; MeCN up to total volume 5 mL; 60 °C.
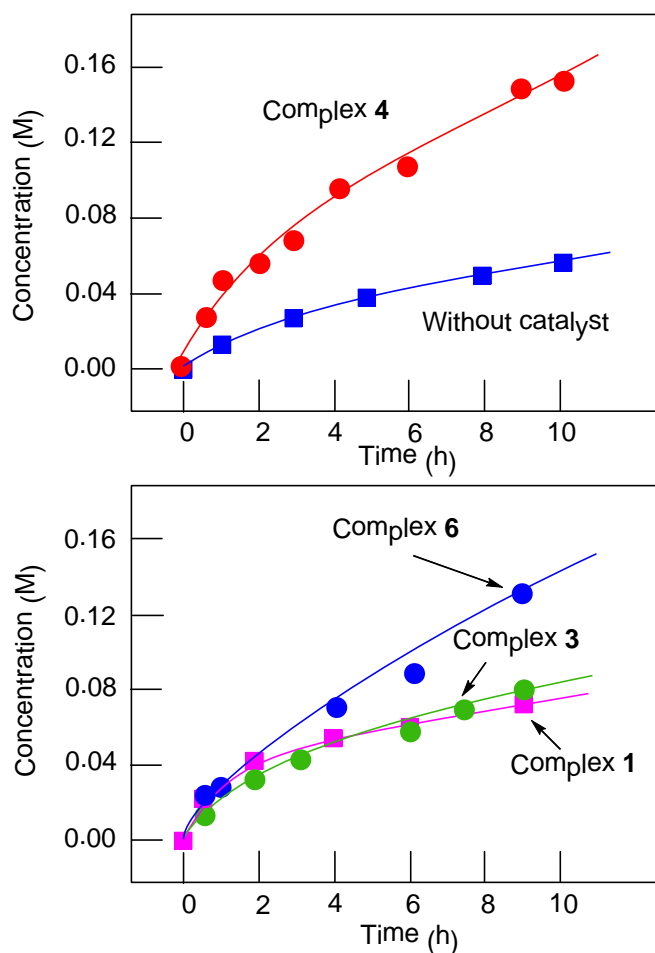
Figure 9. Oxygenation of cyclohexene with the TBHP/Re complex/CH_3CN–H_2O system. Kinetic curves of accumulation of oxygenates in the presence and in the absence of complexes **1**, **3**, **4** and **6** are shown. Conditions [Re catalyst]$_0$ = 2.0×10^{-4} M; [TBHP]$_0$ = 1.4 M (70% aqueous); [cyclohexene]$_0$ = 0.3 M; MeCN up to total volume 5 mL; 60 °C.
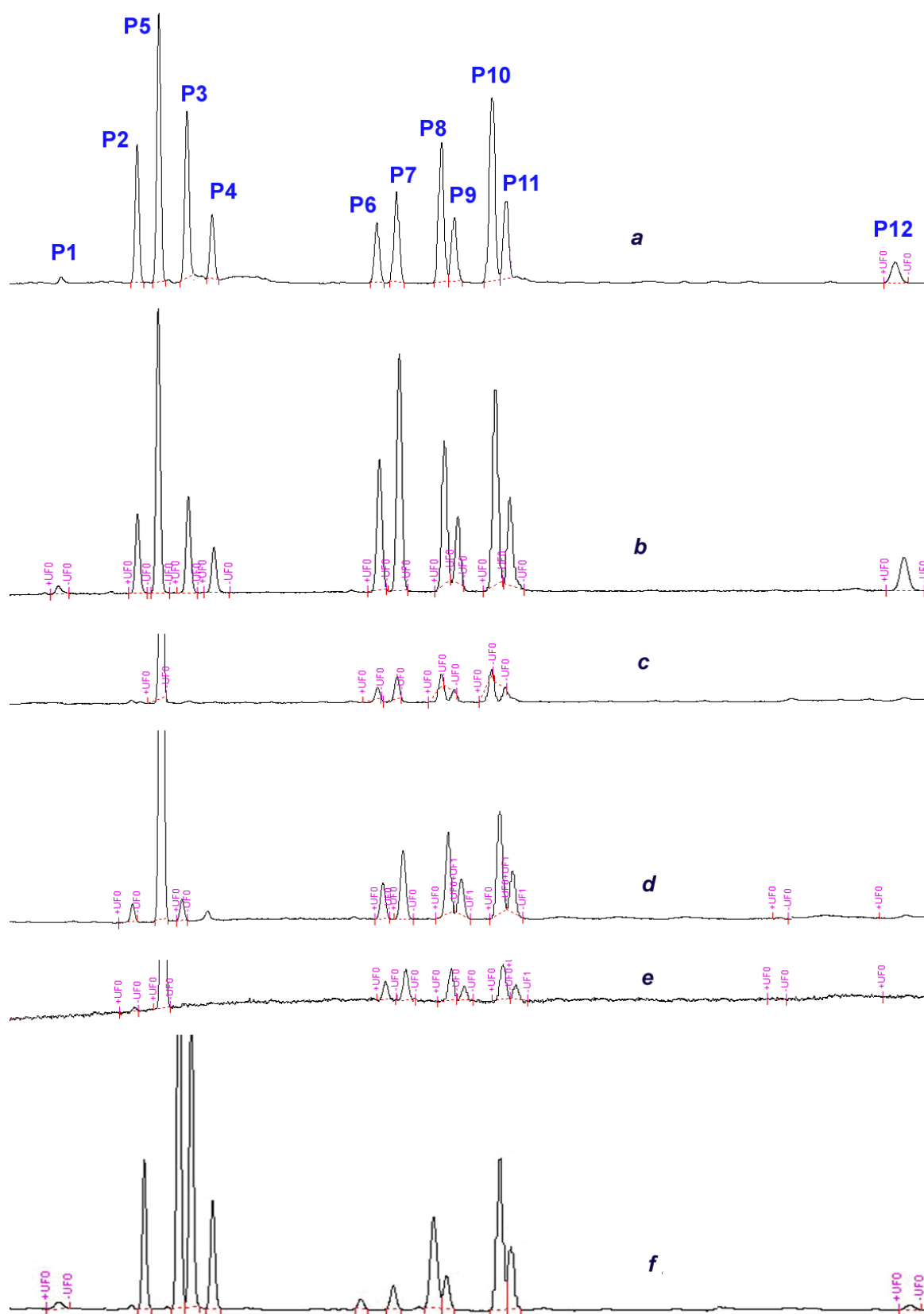
Figure 10. Chromatograms of the reaction mixtures obtained in the methylcyclohexane oxidation (after reduction with PPh$_3$). *a*: Oxidation with H$_2$O$_2$ catalyzed by complex **4** (this work; see also Table 8). *b*: Oxidation with H$_2$O$_2$ catalyzed by Os$_3$(CO)$_{12}$ in the presence of pyridine (for comparison; see Ref. 13d). *c*: Oxidation with TBHP catalyzed by complex **4** (this work; see also Table 8). *d*: Oxidation with TBHP catalyzed by complex **6** (this work; see also Table 8). *e*: Oxidation with TBHP catalyzed by complex **1** (this work; see also Table 8). *f*: Oxidation with TBHP catalyzed by complex [O⊂Cu$_4${N(CH$_2$CH$_2$O)$_3$}$_4$(BOH)$_4$][BF$_4$]$_2$ (for comparison; see Refs. 30i,j,l).
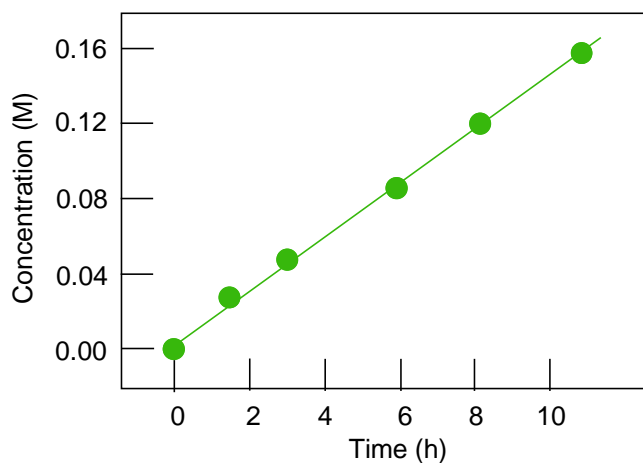
Figure 11. Accumulation of cyclooctanone in the oxygenation of cyclooctanol with the TBHP/**4**/CH$_3$CN–H$_2$O system. Conditions [catalyst **4**]$_0$ = 2.0 × 10^{-4} M; [TBHP]$_0$ = 1.4 M (70% aqueous); [cyclooctanol]$_0$ = 0.25 M; MeCN up to total volume 5 mL; 70 °C.